

https://dspace.org/

Gene expression profiling in human endometrial cells during hormonal stimulation

Wiid, Kyle

2019
https://hdl.handle.net/10539/29791

Downloaded from a DSpace repository. https://dspace.org/

GENE EXPRESSION PROFILING IN HUMAN ENDOMETRIAL CELLS DURING HORMONAL STIMULATION

Kyle Wiid (540501)

Supervisor: Mrs Aleksandra Jovanovic

Supervisor: Professor Raquel Duarte

A Dissertation submitted to the Faculty of Health Sciences, University of the Witwatersrand, Johannesburg, in fulfilment of the requirements for the degree of Master of Science by Dissertation

October 14, 2019

Johannesburg

Declaration



I Kyle Daniel Wiid (Student number: 540501) am a student registered for the degree of Masters (MSc) by Dissertation in the academic year of 2019.

I hereby declare the following:

- I am aware that plagiarism (the use of someone else's work without their permission and/or without acknowledging the original source) is wrong.
- I confirm that the work submitted for assessment for the above degree is my own unaided work except where I have explicitly indicated otherwise.
- I have followed the required conventions in referencing the thoughts and ideas of others.
- I understand that the University of the Witwatersrand may take disciplinary action against me if there is a belief that this is not my own unaided work or that I have failed to acknowledge the source of the ideas or words in my writing.
- I have included as an appendix a report from "Turnitin" (or other approved plagiarism detection) software indicating the level of plagiarism in my research document.

Signature: _____ ____ Date: 15 October 2019

Abstract

The menstrual cycle is a complex system of dynamically interacting hormones, growth factors, cytokines and cells. The cycle is regulated by the combined effects of both the 17β-oestradiol (E_2) and progesterone hormones. An in-depth understanding of complex systems can be obtained if all of the processes that constitute the system are evaluated individually. Therefore, this study aimed to assess the individual effects of both E_2 and medroxyprogesterone acetate (MPA) on human endometrial stromal cells (HESCs) *in vitro*. The effects of these hormones on the expression of *ESR-α*, *PGR*, *TGF-β_1* and *VEGF A* was assessed using Real-Time qRT-PCR, and the secretion of *VEGF A* and *IL-6* was assessed using ELISA. A successful and financially feasible methodology for the isolation of HESCs using endometrial biopsies was established. The cryopreservation technique used in this study resulted in low cell viability, and the data could not be statistically validated. However, the results do show similarities to published data. In the presence of E_2, *ESR-α* expression was minimally altered, and *PGR* expression was minimally increased. Additionally, an increase in growth factor expression was observed. *VEGF A* was upregulated in the presence of both E_2 and MPA, whereas *TGF-β_1* was only upregulated in the presence of E_2. Despite the fact that the data could not be statistically validated, the study provides valuable insight into the individual actions of E_2 and MPA on the menstrual cycle. Furthermore, the study highlights the importance of cryopreservation in the discipline of cell culture.

I dedicate this work to those I love most:

To my mother, Mirella Wiid, I never needed the guidance of a father growing up because I had you as my role model and you gave me all I could ever need as a young man

To my sister, Kimberley Wiid, the only reason I could see so far is because I was standing on the shoulder of a giant

To my girlfriend, Amy, the future belongs to us. Let us make history

To my brother Jake, a brother lost, a brother gained

My Nonna, Mara Molino, I learn new things from you everyday

"When something is important enough, you do it even if the odds are not in your favour"

- Elon Musk

Acknowledgements

Mrs Aleksandra Jovanovic for her supervision and guidance given to me over these 3 years.

Professor Raquel Duarte for her sound supervision and absolute dedication towards assisting in my research.

Doctor Caroline Dickens for all the time spent helping me gain an understanding of many of the techniques needed to be a successful scientist.

Miss Therese Dix-Peek for her willingness to take the time to answer any questions that I asked.

Mrs Hasiena Ali for all her time and effort.

Miss Kimberley Wiid for her unwavering support and critical mind.

Mr Jake Zondagh for all his assistance and support during writing up.

Doctor Lawrence Gobetz and the staff at Vitalab for the assistance with tissue collection.

The patients from Vitalab who so graciously agreed to participate in this research.

Doctor Tanya Augustine for the use of her TC20 cell counter.

Professor Raquel Duarte and Mrs Aleksandra Jovanovic for the funding of this research.

The NRF for their funding.

My entire family for bearing with me through this.

Conference outputs

Molecular Biosciences Research Thrust, Johannesburg, 2017. *Poster*. “Isolation of Human Endometrial Stromal Cells: A Methodology.” Kyle Wiid, Aleksandra Jovanovíc and Raquel Duarte.

Table of contents

Declaration i

Abstract ii

Acknowledgements iv

Conference outputs v

List of abbreviations ix

Reference Sequence Database x

List of figures xii

Chapter 1: Introduction 1

1.1. The menstrual cycle 1

1.2. Hormones involved in the menstrual cycle 1

1.2.1. Oestrogen 1

1.2.1.1. The oestrogen receptor 2

1.2.2. Progesterone 4

1.2.2.1. The progesterone receptor 5

1.3. Human endometrial stromal cells (HESCs) 6

1.4. Cytokines affected by hormonal stimulation 8

1.4.1. *Transforming growth factor β* (*TGF-β*) 8

1.4.2. *Vascular endothelial growth factor* (*VEGF*) 8

1.4.3. *Interleukin-6* (*IL-6*) 9

1.5. Aim and objectives 10

Chapter 2: Experimental Procedures 11

2.1. Ethical considerations 11

2.2. Tissue collection 11

2.3. Human endometrial stromal cell isolation 11

2.4. Sample storage 12

2.5. Cell counts and viability 12

2.6. Hormonal stimulation 13

2.7. RNA Extraction 13
2.8. RNA precipitation 14
2.9. complementary deoxyribonucleic acid (cDNA) synthesis 14
2.10. Primer design 15
2.11. Real-Time Quantitative Reverse Transcription PCR (Real-Time qRT-PCR) 15
2.12. Enzyme-linked immunosorbent assay (ELISA) 16
2.13. Statistical analysis 17
Chapter 3: Results 19
3.1. Human endometrial stromal cells (HESCs) 19
3.1.1. Predisposition to microbial infection 19
3.1.2. Presence of blood during isolation procedure 19
3.1.3. Morphology *in vitro* 20
3.1.3.1. Morphology after 24 – 48 hours 20
3.1.3.2. Morphology after 72 – 96 hours 20
3.1.3.3. Confluency after 192 – 240 hours 23
3.2. Human endometrial stromal cell (HESC) viability 23
3.2.1. Post-cryopreservation 23
3.2.2. Troubleshooting 25
3.2.3. Viability counts 25
3.2.3.1. Patient 1 28
3.2.3.2. Patient 2 28
3.2.3.3. Patient 3 28
3.2.3.4. Patient 4 32
3.2.3.5. Patient 5 32
3.3. Real-Time Quantitative Reverse Transcription PCR (Real-Time qRT-PCR) setup and analysis 35
3.3.1. Primer Design 35
3.3.2. Primer Analysis 35
3.3.3. RNA Isolation 35

3.3.4. RNA Precipitation 35
3.3.5. Real-Time Quantitative Reverse Transcription PCR (Real-Time qRT-PCR) Analysis 39
3.3.5.1. Reference Genes 39
3.3.5.2. Oestrogen receptor α (*ESR-α*) 39
3.3.5.3. Progesterone receptor (*PGR*) 42
3.3.5.2. *Transforming growth factor β* (*TGF-β*$_1$) 42
3.3.5.4. *Vascular endothelial growth factor* A (*VEGF A*) 42
3.4. Enzyme-linked immunosorbent assays (ELISAs) 46
3.4.1. *Interleukin-6* (*IL-6*) 46
3.4.2. *Vascular endothelial growth factor* A (*VEGF A*) 46
3.5. Statistical Analysis 46
3.5.1. Real-Time Quantitative Reverse Transcription PCR gene expression 46
3.5.2. Spearman rank correlation 46
Chapter 4: Discussion 51
4.1. Establishment of Human endometrial stromal cell lines as a successful *in vitro* model 51
4.2. Factors affecting cell viability 53
4.3. The importance of primer design in Real-Time Quantitative Reverse Transcription PCR (Real-Time qRT-PCR) 55
4.4. E_2 and MPA on receptor expression 56
4.5. E_2 and MPA on growth factor expression 57
4.6. Conclusion 58
APPENDIX 60
Appendix A: Ethical clearance certificate (M1511106) 61
Appendix B: Blank consent form 62
Appendix C: PBS Stock Solution 65
Appendix D: Primer Design 66
References 83

List of abbreviations

BLAST	Basic Local Alignment Search Tool
BMP	bone morphogenic proteins
BSA	bovine serum albumin
°C	degrees Celsius
cDNA	complementary deoxyribonucleic acid
CF	correction factor
cm	centimetre
Cq	quantitation cycle
D&C	Dilation and Curettage
DMSO	dimethyl sulfoxide
DNA	deoxyribonucleic acid
DNase	deoxyribonuclease
dNTP	deoxynucleotide
E_1	oestrone
E_2	17beta-oestradiol
E_3	oestriol
EDTA	ethylenediaminetetraacetic acid
ELISA	enzyme-linked immunosorbent assay
ESR	oestrogen receptor
ESR-α	oestrogen receptor alpha
ESR-β	oestrogen receptor beta
FCS	foetal calf serum
H_2O	water
HESC	human endometrial stromal cell
HREC	Human Research Ethics Committee
HRP	horseradish peroxidase
IGFBP-1	insulin-like growth factor binding protein-1
IL-6	*interleukin-6*
LH	luteinising hormone
M	molar
MIQE	Minimum Information for Publication of Quantitative Real-Time PCR Experiments
ml	millilitre

mM	millimolar
mm	millimetre
MPA	medroxyprogesterone acetate
mRNA	messenger ribonucleic acid
NCBI	National Center for Biotechnology Information
ng	nanogram
nm	nanometre
NRQ	normalised relative quantification
NTC	no template control
ρ	rho
P450scc	cholesterol side-chain cleavage enzyme
PBS	Dulbecco's phosphate buffered saline
PCR	polymerase chain reaction
PDGF	platelet-derived growth factor
PF4	platelet factor 4
pg	picogram
PGR	progesterone receptor
PRL	prolactin
Real-Time qRT-PCR	Real-Time Quantitative Reverse Transcription PCR
RefSeq	Reference Sequence Database
RLT	lysis buffer
RNA	ribonucleic acid
RNase	ribonuclease
RPE	wash buffer
RPMI-1640	Roswell Parks Memorial Institute 1640
RT	reverse transcriptase
RW1	wash buffer
SYBR	fluorescent dye
TGF-β	transforming growth factor beta
TGF-β1	*transforming growth factor beta 1*
*TGF-β*2	*transforming growth factor beta 2*
*TGF-β*3	*transforming growth factor beta 3*
UBC	*ubiquitin C*
UDG	uracil-DNA-glycosylase
µg	microgram

µl	microlitre
µm	micrometre
VEGF	*vascular endothelial growth factor*
Vg-1	vitellogenin-1
VPF	vascular permeability factor
YWHAZ	*tyrosine 3-monooxygenase/tryptophan 5-monooxygenase activation protein zeta*

List of figures

Figure 1: Biosynthesis of the major androgens 3
Figure 2: Cell colonies from human endometrial samples present in vitro 48 hours post-isolation 21
Figure 3: Cell colonies from human endometrial samples present in vitro 72 hours post-isolation 22
Figure 4: Cell colonies from human endometrial samples present in vitro 240 hours post-isolation 24
Figure 5: Mean cell counts of patients 26
Figure 6: Individual cell counts for patient 1 29
Figure 7: Individual cell counts for patient 2 30
Figure 8: Individual cell counts for patient 3 31
Figure 9: Individual cell counts for patient 4 33
Figure 10: Individual cell counts for patient 5..... 34
Figure 11: Primer efficacy Cq values of (A) *TGF-β_1*, (C) *ESR-α*, (E) *PGR* and (G) *VEGF A* and the Melting Temperatures of (B) *TGF-β_1*, (D) *ESR-α*, (F) *PGR* and (H) *VEGF A*. 37
Figure 12: Normalised relative quantities of *ESR-α* 41
Figure 13: Normalised relative quantities of *PGR*..... 43
Figure 14: Normalised relative quantities of *TGF-β*1..... 44
Figure 15: Normalised relative quantities of *VEGF A*..... 45
Figure 16: Five-parameter logistic curve expressing to concentration of *IL-6* 47
Figure 17: Five-parameter logistic curve expressing to concentration of *VEGF A*..... 48

List of tables

Table 1: Mean percentage of living cells in Patients 1 – 5 26
Table 2: Designed primers for *TGF-β*1, *TGF-β*1, *TGF-β*1, *ESR-α, ESR-β, PGR* and *VEGF A* 36
Table 3: Cq and melting temperature of analysed genes 38
Table 4: Mean Cq and Melting Temperatures for *UBC* and *YWHAZ* genes 40
Table 5: Data for ρ calculation for the correlation of the percentage of live cells with the percentage of genes expressed 49
Table 6: Data for ρ calculation for the correlation of the total live cell count with the percentage of genes expressed 50

Chapter 1: Introduction

1.1. The menstrual cycle

The endometrium is the final target for hormonal signals originating from the hypothalamic-hypophyseal-ovarian axis (Tabibzadeh, 1998) and these signals ultimately result in the menstrual cycle. The menstrual cycle, which has a median duration of 28 days, is divided into three distinct phases: menstruation, proliferative, and secretory (Deligdisch, 2000). The proliferative phase is initiated through the release of oestrogen from the ovaries (Deligdisch, 2000). The increased levels of oestrogen results in the proliferation and growth of cells within the endometrium (Deligdisch, 2000). In response to the prolonged increased concentration of oestrogen, the anterior pituitary secretes luteinising hormone (LH) resulting in an LH surge (Gibson and Hammoud, 2013). The surge in LH initiates the ovulation process, releasing a follicle from one of the ovaries. Following ovulation, a remnant of the follicle still present in the ovary differentiates into the corpus luteum. The corpus luteum contains cells which begin secreting progesterone (Gibson and Hammoud, 2013). The presence of progesterone influences further priming within the endometrium and the changes which occur result in the secretory phase of the menstrual cycle (Gibson and Hammoud, 2013).

1.2. Hormones involved in the menstrual cycle

1.2.1. Oestrogen

Endogenous oestrogens are naturally occurring steroid hormones present in both males and females. In women, this hormone is essential in both the hypothalamic-hypophyseal-ovarian axis (Tabibzadeh, 1998) as well as in ancillary sexual characteristics (Santoro *et al.*, 2016).

The female body produces three endogenous oestrogens which are derived from the cleavage of cholesterol, namely oestrone (E_1) (Figure 1), 17β-oestradiol (E_2) (Figure 1) and oestriol (E_3). These hormones are produced in different regions of the body and function locally as well as throughout the body (Gruber *et al.*, 2002). E_2, derived from the aromatisation of testosterone, is synthesised within the ovaries by the theca and granulosa cells, as well as the luteinised forms of these cells (Ryan, 1982). E_1 and E_3, derived from the aromatisation of androstenedione and 16α-hydroxytestosterone respectively, are predominantly formed within the liver through

the metabolism E_2 (Gruber *et al*., 2002). Of these three oestrogens, E_2 is the most potent, acting both locally within the ovaries, as well as within the uterus. During the menstrual cycle, E_2 is secreted from the granulosa cells within the ovary to initiate the proliferative phase and eventual LH surge which results in both ovulation and the luteinisation of the theca and granulosa cells (Deligdisch, 2000). Luteinisation of these cells results in the formation of the corpus luteum and the secretion of progesterone (Gibson and Hammoud, 2013).

1.2.1.1. The oestrogen receptor

Oestrogen receptors (ESRs) are a group of ligand-activated receptors which form part of the nuclear hormone receptor superfamily. These receptors consist of three clearly defined structural domains: an NH_2-terminal (A/B) domain, the C Deoxyribonucleic acid (DNA) binding domain, and the ligand binding (D/E/F) domain (Nilsson *et al.*, 2001). Within the body there are two distinct and identifiable forms of ESRs, namely oestrogen receptor alpha (ESR-α) and oestrogen receptor beta (ESR-β) and the differences of which, at the amino acid level, are dependent on the domain. The DNA binding domain of both ESRs is highly homologous (97%); however, major differences occur within the other two domains where the ligand binding domain and the NH_2- terminus is 56% and 24% homologous respectively (Dahlman-Wright *et al.*, 2006).

The ligand binding domains of ESR-α and ESR-β display a similar affinity to endogenous oestrogens such as E_2, despite their poor homogeneity (56%) (Kuiper *et al.*, 1997). However, their tissue expression patterns differ markedly. *ESR-α* shows much larger mRNA expression within the endometrium, cervix, vagina and breast, whereas *ESR-β* has shown a greater mRNA expression within the ovaries, spleen, hypothalamus, thymus and lungs (Couse *et al.*, 1997). In addition to its expression within whole tissues, ESR-α is present within endothelial cells (Trenti *et al.*, 2018). Evidence suggests that this receptor assists E_2 with increasing both the migration and proliferation of endothelial cells, both important factors required for angiogenesis (Simoncini *et al.*, 2006).

Immunostaining has confirmed that *ESR-α* is prominently expressed during the proliferative stage of the menstrual cycle in both the epithelial and stromal cells of the endometrium. The receptor remains prominent within both cell types up until the mid- to late- secretory phase where its prominence is only retained within the stromal cell compartment (Classen-Linke *et al.*, 1998). The activation of *ESR-α* through E_2 within the endometrium plays a vital role in

ensuring the progression of the menstrual cycle, which is achieved through the upregulation of progesterone receptor expression (Kastner *et al*., 1990).

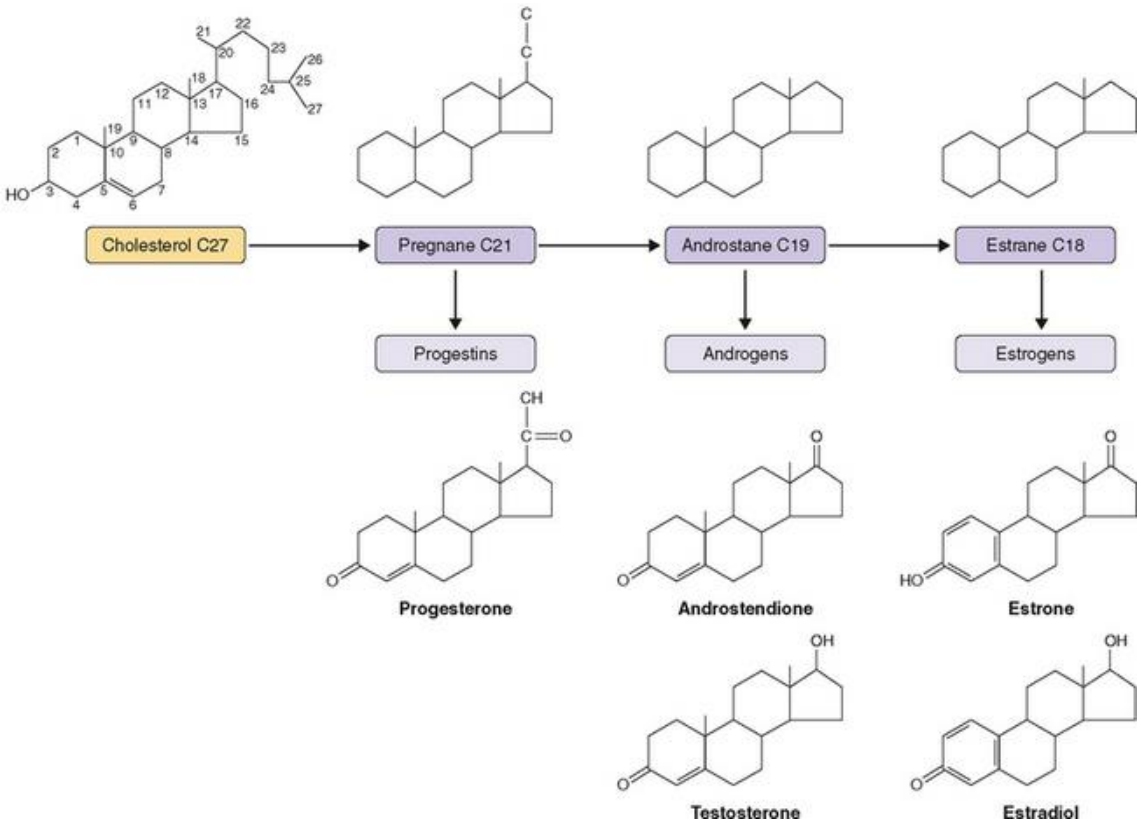


Figure 1: Biosynthesis of the major androgens

The 27-carbon cholesterol molecule is the precursor to the progestins, androgens and oestrogens (estrogen). Image taken from Gupta and Chia, (2013).

1.2.2. Progesterone

Progesterone is an endogenous hormone primarily produced following ovulation and the formation of the corpus luteum. Low concentrations of this hormone are also produced and secreted by the adrenal glands of women (King and Brucker, 2011). The function of progesterone is in the regulation of normal female reproductive processes such as the growth and maintenance of the uterine endometrial lining during the secretory phase, the support of blastocyst implantation, the maintenance of the early stages of pregnancy and the lobular and alveolar development of the mammary gland (Clarke and Sutherland, 1990). Therefore, the primary role of progesterone is the maintenance of normal female reproductive processes. Additionally, progesterone has been shown to be essential in the prevention of osteoporosis (Balasch, 2003) as well as having a neurosteroidal function in the brain (Genazzani *et al.*, 2000).

Progesterone belongs to the steroid hormone class of progestogens. Progestogens are divided into endogenous progestogens and progestins, with the latter encompassing all synthetic compounds which act on progesterone receptors (King and Brucker, 2011). Medroxyprogesterone acetate (MPA) is one example of a progestin. MPA is a synthetic progestin compound used as an oral contraceptive and in hormone replacement therapy (Ghatge *et al.*, 2005). It has been found that this progestin can mimic the effects of regular progesterone regarding its gene expression profile (Ghatge *et al.*, 2005). Progesterone is the principal type of endogenous progestogen and like other progestogens is characterised by its pregnane (21-carbon) skeleton (Al-Asmakh, 2007).

The precursor of progesterone is cholesterol, and its synthesis occurs within the corpus luteum where cholesterol side-chain cleavage enzyme (P450scc) and 3β-hydroxysteroid dehydrogenase catalyse the pathway converting cholesterol into progesterone (Figure 1) (Kamada *et al.*, 1997).

During the menstrual cycle, the formation of the corpus luteum and the conversion of theca and granulosa cells into their lutein counterparts, enables the production and secretion of progesterone (Ross and Pawlina, 2006). The secretion of progesterone signifies the start of the secretory phase of the menstrual cycle (Ross and Pawlina, 2006).

1.2.2.1. The progesterone receptor

Progesterone Receptors (PGRs) belong to the superfamily of DNA-binding receptors (Baulieu, 1991). These receptors have four distinct domains: an N-terminal transcription domain, a centrally placed DNA binding domain, a hinge region and a C-terminal ligand binding domain (Baulieu, 1991). The PGR is found in two dominant distinct molecular forms: PGR-A and PGR-B, with PGR-B being 164 amino acids longer than PGR-A (McDonnell and Goldman, 1994). Numerous other PGRs have been described such as PGR-C, PGR-M, and PGR-S; however, none of these alternative PGRs have been proven to be expressed at physiologically acceptable concentrations *in vivo* (Samalecos and Gellersen, 2008).

Progesterone functions by binding to both PGR-A and PGR-B, and even though both receptors act indistinguishably by allowing for the binding of progesterone, the downstream effect of these two receptors is markedly different. In mice, it has been shown that PGR-A acts predominantly on ovarian and uterine function, while PGR-B is essential in the development of the mammary gland (Mulac-Jericevic and Conneely, 2004). Studies suggest that when bound to a ligand PGR-A functions as an inhibitory molecule (Vegeto *et al.*, 1993). When bound to a ligand, the receptor has shown little transcriptional activity but rather curtails other steroid receptors, including PGR-B and ESRs (Vegeto *et al.*, 1993).

Within the endometrium, the expression of both PGR-A and PGR-B is dependent on the stages of the menstrual cycle as well as the cell type. PGR-A is highly expressed in human endometrial stromal cells (HESCs) throughout all three stages of the menstrual cycle. In comparison, the expression of PGR-A within epithelial cells of the endometrium decreases as the secretory phase progresses (Mote *et al.*, 1999). In contrast, the expression of PGR-B peaks during the mid-proliferative phase of the menstrual cycle in both HESCs and epithelial cells and then gradually declines as the menstrual cycle progresses (Jabbour and Critchley, 2001). Due to its permanency in expression during the menstrual cycle, PGR-A is suggested to be the dominant of the two receptor isoforms within HESCs (Mote *et al*., 1999). It has also been found that PGR-A plays a larger role in the transactivation of decidual prolactin promoters within stromal cells (Gao *et al*., 2000).

The functional and the basal layer form the two distinct regions of the endometrium (Ross & Pawlina, 2006). Changes within the functional layer of the endometrium are most evident during the menstrual cycle. The cells associated with the endometrium, experience an increased

level of growth, proliferation and differentiation (Ross & Pawlina, 2006). One cell type which undergoes such changes is HESCs (Ross & Pawlina, 2006).

1.3. Human endometrial stromal cells (HESCs)

The origin of tissue culture is deeply embedded in a period of scientific discovery which saw a wealth of many developmental models proposed by scientists such as Wilhelm Roux and August Weismann (Sander and Schneider, 1991). In 1885 Roux successfully removed the medullary plate of a chick embryo and maintained it in a warm saline solution for days (Gruber and Jayme, 1994). Even though this experiment was a far cry from cell and tissue culture, it laid the groundwork for the ideology of cell culturing to be used as an *in vitro* model of experimentation (Gruber and Jayme, 1994). At the turn of the twentieth century, a methodology for the study of animal cells *in vitro* was devised by Harrison *et al.* (1907). Harrison (1907) successfully managed to isolate developing nerve fibres from frog embryos and keep these fibres alive in lymph from an adult frog for upwards of a week. It was also found that these developing nerve fibres continued to grow within the lymph until they died. Harrison's discovery allowed for cells and tissues to be studied without the variations which may arise within *in vivo* models (Freshney, 2005).

The ability to study cells *in vitro* was transposed to the study of normal uterine cells in the late 1960's (Luginbuhl, 1968) and it was not until 1979 that a fixed methodology for the isolation of human endometrial cells was established (Satyaswaroop *et al.*, 1979). Satyaswaroop *et al.* (1979) managed to not only isolate endometrial glands from uterine tissue but described a method that depicted stromal cell isolation as well. Since then, many methodologies published regarding the isolation of cells from the human endometrium have been based on the work conducted by Satyaswaroop *et al.* (1979) (Varma *et al.*, 1982; Fernandez-Shaw *et al.*, 1992; Arnold *et al.*, 2001). Research in the field of reproductive biology was significantly improved with the successful isolation of the Ishikawa cell line. The Ishikawa cell line is a well-differentiated endometrial adenocarcinoma cell line, which is positive for the presence of both oestrogen and progesterone receptors (Nishida *et al.*, 1985; Nishida, 2002). Even though Ishikawa cells have a tendency to transform into undifferentiated cells after long-term culture, they still represent a good *in vitro* model for numerous research opportunities in reproductive biology (Nishida, 2002).

HESCs are fibroblasts found within the endometrium. The origin of these cells is unclear, however, research indicates that these cells may potentially differentiate from endometrial

mesenchymal stem cells (Spitzer *et al.*, 2012), which themselves originate from bone marrow-derived mesenchymal stem cells (Aghajanova *et al.*, 2010). HESCs are influenced by the ovarian steroid hormones, oestrogen and progesterone, which alter the cells structurally and functionally (Ren *et al.*, 2015). Observations have been made that progestins such as MPA alter these cells in a similar way (Vereide *et al.*, 2006; Ren *et al.*, 2015). During the menstrual cycle, these cells undergo a process known as decidualisation (Dunn *et al*., 2003; Aghajanova *et al.*, 2010), which is characterised by a series of morphological and biochemical alterations (Gellersen and Brosens, 2003).

The process of decidualisation of the stromal cells is a result of the initial priming of these cells by E_2, and then the action of both E_2 and progesterone in a time-dependent manner during the menstrual cycle (Logan *et al.*, 2013). These differentiated endometrial stromal cells (decidual stromal cells) become rounded, acquire myofibroblast characteristics and secrete a variety of cytokines including prolactin (PRL) and insulin-like growth factor binding protein-1 (IGFBP-1) (Tabanelli *et al*., 1992). These stromal cells also undergo a series of molecular changes, which lead to altered steroid hormone receptor expression, extracellular matrix and cytoskeleton remodelling as well as altered gene expression (Brar *et al.*, 2001). During the menstrual cycle it has been found that stromal cell decidualisation is initiated at the start of the secretory phase (Dunn *et al.*, 2003). Stromal cells begin to decidualise around spiral arteries within the functional layer of the endometrium (Kajihara *et al.*, 2013). This differentiation extends throughout the functional layer of the endometrium until all stromal cells within this layer are decidual (Kajihara *et al.*, 2013). In the absence of pregnancy, the functional layer within the endometrium becomes ischemic and decidual cells are sloughed off during menstruation (Gellersen and Brosens, 2003). However, when blastocyst attachment occurs, and pregnancy proceeds, the decidual reaction extends into the basal layer of the endometrium (Brosens *et al.*, 2002; Gellersen and Brosens, 2003). The extension of the decidual reaction into the basal layer is essential for both trophoblast invasion and placentation (Brosens *et al.*, 2002).

The effect of hormonal stimulation on HESCs, such as those seen in decidualisation, is not limited to morphological alterations. HESCs are molecularly altered during hormonal stimulation, which results in the differential expression of cytokines, hormones and their receptors (Tabanelli *et al.*, 1992). Several cytokines such as transforming growth factor beta (*TGF-β*) (Stoikos *et al.*, 2008), vascular endothelial growth factor (VEGF) (Zhang *et al.*, 1995; Huang *et al.*, 1998), and interleukin-6 (IL-6) (Tabibzadeh *et al.*, 1989) are affected by the hormonal stimulation of HESCs.

1.4. Cytokines affected by hormonal stimulation

1.4.1. Transforming growth factor β (TGF-β)

TGF-βs are dimeric, disulphide linked peptides which belong to the Transforming growth factor β superfamily. With the exception of TGF-βs, this superfamily consists of inhibins, activin, bone morphogenic proteins (BMPs), anti-Müllerian hormone, decapentaplegic and vitellogenin-1 (Vg-1). There are five recognised isoforms of TGF-β (TGF-β_{1-5}) found within this superfamily of which three (TGF-β_{1-3}) are present within mammals (Massagué *et al.*, 1992). TGF-β isoforms, within the endometrium of humans, have been implicated in regulating normal endometrial function, the regulation of decidualisation and placental development and function (Jones *et al.*, 2006b).

Due to the involvement of TGF-βs in the tissue proliferation and remodelling process, the isoforms of TGF-β found within humans (TGF-β_{1-3}) are differentially expressed in the endometrium (Gold *et al.*, 1994). It has been found that within the endometrium of humans, TGF-β_2 is predominantly localised to the endometrial stromal compartment, whereas TGF-β_1 and TGF-β_3 are found in stromal cells and within luminal epithelial cells (Gold *et al.*, 1994). Within the human endometrium, it has been shown that TGF-β_1 expression is regulated by E_2 stimulation (Takahashi *et al.*, 1994).

1.4.2. *Vascular endothelial growth factor* (*VEGF*)

VEGF is a platelet-derived growth factor which belongs to the super-gene family VEGF-Platelet-derived growth factor (-PDGF). Initially described as vascular permeability factor (VPF) (Senger *et al.*, 1983), varying forms of this molecule have been identified in a multitude of organisms, leading to the inclusion of the suffix A (VEGF A) when described in humans (Mattei *et al.*, 1996).

The endometrium of humans is host to a complex and dynamic vasculature, which is influenced by the cyclical hormonal changes throughout the menstrual cycle (Girling and Rogers, 2009). During the menstrual cycle, VEGF A is essential in the remodelling process of the endometrial vasculature through angiogenesis (Girling and Rogers, 2005), lymphangiogenesis (Koukourokis *et al.*, 2005) and vascular maturation (Fraser *et al.*, 2008). HESCs have exhibited alterations in *VEGF A* expression in response to hormonal stimulation. There are multiple studies which report an upregulation of *VEGF A* messenger ribonucleic acid (mRNA) expression in response to either E_2 (Huang, Liu and Dawood, 1998; Classen-Linke *et al.*, 2000)

or progesterone (Zhang, Rees and Bicknell, 1995) treatment. This implies an essential regulatory role of these hormones in ensuring menstrual cycle progression through the control of the endometrial vasculature (Girling and Rogers, 2009).

1.4.3. *Interleukin-6* (*IL-6*)

IL-6 is a long chain α-helix bundle protein from the hematopoietin cytokine family (Bazan, 1990). This pleiotropic cytokine is involved in several biological processes such as immunoregulation, hematopoiesis and inflammation (Kishimoto, 2010).

Through the regulation of immunity and inflammation within the endometrium, IL-6 ensures a highly controlled environment allowing for blastocyst attachment and immunosurveillance (Hunt, 2006). This cytokine shows cyclical expression during the menstrual cycle (Von Wolff *et al.*, 2002), partly due to the regulatory roles of the ovarian hormones oestrogen and progesterone. E_2 (Tabibzadeh *et al.*, 1989) and progesterone (Kim *et al.*, 2012), inhibit the expression of *IL-6* which promotes a non-inflammatory environment.

1.5. Aim and objectives

The menstrual cycle is a complex system of dynamically interacting hormones, growth factors, cytokines and cells controlled by its regulatory hormones. The complexity of this system is a direct result of the role of the uterus in pregnancy. Therefore, the menstrual cycle is crucial in ensuring successful pregnancy. The menstrual cycle is highly regulated by oestrogen and progesterone, which act in unison to induce responses that are pivotal for the progression of the menstrual cycle.

Research efforts from multiple studies have focussed on understanding the complex regulation of the menstrual cycle. However, the most successful way to understand the dynamics of such an intricate system is to gain a deeper understanding of the individual processes that constitute the system. Therefore, an investigation into the independent roles of oestrogen and progesterone will add valuable insight into the combined action of the two steroid cycle hormones, which will supplement the expanding knowledge base on hormonal regulation during the menstrual cycle.

The aim of this research is to understand the individual functions of oestrogen and progesterone in receptor expression and cytokine profiles within human endometrial stromal cells.

The specific objectives of this study were to:

- Isolate HESCs.
- Prove successful isolation of HESCs through light microscopy.
- Test the viability of the HESCs.
- Hormonally stimulate the HESCs with E_2 and MPA.
- Assess the effect of E_2 and MPA on the expression of E_2 and MPA receptors in HESCs using real-time polymerase chain reaction (Real-Time qRT-PCR).
- Assess the effect of E_2 and MPA on *TGF-*β_1 expression in HESCs using Real-Time qRT-PCR.
- Assess the effect of E_2 and MPA on *VEGF* A expression in HESCs using Real-Time qRT-PCR and an enzyme-linked immunosorbent assay (ELISA).
- Assess the effect of E_2 and MPA on *IL-6* expression from HESCs using an ELISA.

Chapter 2: Experimental Procedures

2.1. Ethical considerations

The use of the endometrial tissue was in accordance with the Human Research Ethics Committee – Medical (HREC – Medical), University of the Witwatersrand, Johannesburg, South Africa (Clearance certificate number: M1511106) (see Appendix A).

2.2. Tissue collection

Endometrial biopsies were obtained from 5 healthy, reproductively active women undergoing dilation and curettage (D&C), following informed consent (see Appendix B). The female patients had no clinical history of hormonal dysfunction, or any infectious or malignant endometrial disease. Endometrial biopsies obtained were in the secretory phase of the menstrual cycle. Biopsied tissue was transported from Vitalab to the laboratory at Wits Medical School on ice. Roswell Parks Memorial Institute (RPMI) 1640 culture medium, containing L-glutamine (Lonza), 5% foetal calf serum (FCS) and 0.2% Penicillin-Streptomycin-Amphotericin 100X (Lonza) was used for transportation. Biopsied tissue was stored overnight at 4°C in the aforementioned transport medium.

2.3. Human endometrial stromal cell isolation

The tissue dispersion protocol, and isolation of endometrial stromal cells, was based on a modified version of the procedures conducted by Arnold *et al.* (2001). The entire procedure was carried out in sterile conditions, under a laminar flow hood. Tissue was removed from the transport medium and thoroughly rinsed using Dulbecco's phosphate buffered saline (PBS), pH 7.4 (see Appendix A). Following rinsing, unwanted tissue was discarded, and the remainder was minced into 1 mm^3 pieces. Once minced, the tissue was rinsed in PBS, pH 7.4 and immersed in a RPMI 1640 with L-glutamine (Lonza) and 0.25% collagenase type 1 (Sigma Aldrich) solution. Tissue was incubated for 2 hours in a 37°C shaking water bath, to allow for enzymatic digestion. The tissue digest was vigorously aspirated to ensure that the remaining tissue pieces were broken up. The tissue was then passed over a 100 µm sieve, which retained any glandular tissue and allowed both stromal cells and red blood cells to pass through. Cells which passed through the sieve were centrifuged at 400 x g for 5 minutes and resuspended in 3 ml of growth media containing RPMI 1640 with L-glutamine, 10% FCS and 0.1% Penicillin-

Streptomycin-Amphotericin 100X (Lonza). Red blood cells were removed by layering the cell suspension over 3 ml of Histopaque 1077 (Sigma-Aldrich). The solution was centrifuged at 400 x g for 10 minutes and the white cellular interface was collected. The cellular suspension was rinsed in PBS, pH 7.4, and centrifuged at 400 x g for 5 minutes in a wash step, which was performed twice. Cells were resuspended in 5 ml of growth media containing RPMI 1640 with L-glutamine, 10% FCS and 0.1% Penicillin-Streptomycin-Amphotericin 100X (Lonza). Cells were transferred to a 25 cm^3 culture dish for growth. Once 80% confluency was reached, as verified by light microscopy, the samples were trypsinised in 2 ml 0.25% Trypsin-ethylenediaminetetraacetic acid (-EDTA) (Sigma-Aldrich) for 15 minutes at 37°C. Trypsinisation was halted post-incubation by the addition of 2 ml growth media containing RPMI 1640 with L-glutamine, 10% FCS and 0.1% Penicillin-Streptomycin-Amphotericin 100X (Lonza). The cellular suspension was transferred to a centrifuge tube for centrifugation at 400 x g for 5 minutes. The cellular suspension was rinsed in PBS, pH 7.4, and centrifuged at 400 x g for 5 minutes in a wash step, which was performed twice. Samples were divided into separate samples, and either resuspended in 5 ml growth media containing RPMI 1640 with L-glutamine, 10% FCS and 0.1% Penicillin-Streptomycin-Amphotericin 100X (Lonza) for passaging; or resuspended in 1 ml of freezing media containing RPMI 1640 with L-glutamine, 10% FCS and 10% dimethyl sulfoxide (DMSO) (Sigma-Aldrich) for storage.

2.4. Sample storage

Isolated HESCs were stored at -80°C in 1 ml freezing media, containing RPMI 1640 with L-glutamine, 10% FCS and 10% DMSO (Sigma-Aldrich). Cells were frozen using a Nalgene® Mr. Frosty, which allowed for the incremental freezing of cells at a cooling rate of 1°C every minute. Isolated HESCs were stored at -80°C until sample processing was required. When samples were required, they were thawed at room temperature. Freezing media was diluted in 2 ml PBS, pH 7.4, and centrifuged at 400 x g for 5 minutes. The cellular suspension was rinsed in PBS, pH 7.4, and centrifuged at 400 x g for 5 minutes in a wash step, which was performed twice to ensure the complete removal of DMSO.

2.5. Cell counts and viability

Cells were counted, and viability was established, using the TC20™ Automated Cell Counter (Bio-Rad). Samples were mixed gently, and 20 µl aliquots of the cellular suspension were added to 20 µl of 0.4% trypan blue dye. Aliquotted samples were mixed thoroughly, and 10 µl of each aliquot was pipetted into the cell counting chamber. Cell counts were done in

duplicate in 0.4% trypan blue staining. Counting was completed within 5 minutes, to ensure accuracy of the cell counts. Cell counts for individual samples were separated according to diameter. The mean cell count for each diameter (5-25 µm), mean total cell count, mean live count and the mean live percentage of cells were obtained.

2.6. Hormonal stimulation

One sample for each patient was removed from storage at -80°C, and allowed to incubate at 37°C for 24 hours prior to hormonal treatment. After 24 hours, samples were rinsed in PBS, pH 7.4, and centrifuged at 400 x g for 5 minutes in a wash step, which was performed twice. Each patient sample was divided into two experimental groups and a control group. After division into groups, samples were resuspended in 6 ml growth media containing RPMI 1640 with L-glutamine, 10% FCS and 0.1% Penicillin-Streptomycin-Amphotericin 100X (Lonza) to which either 1 x 10^{-7} M 17β-Oestradiol (Sigma-Aldrich) or 2 x 10^{-7} M Medroxyprogesterone Acetate (Sigma-Aldrich) was added to the experimental groups. Only RPMI 1640 with L-glutamine was added for the control group. Patient samples for each group were then divided into two, and transferred into 6-well culture plates, and allowed to incubate at 37°C for 48 hours. Following incubation, samples were aliquotted and centrifuged at 400 x g for 5 minutes. The supernatant was collected and stored at -80°C for ELISA. Cells were resuspended in 350 µl Buffer RLT (Qiagen) containing 1% β-Mercaptoethanol (Sigma-Aldrich) for RNA extraction.

2.7. RNA Extraction

RNA extraction was done using the RNeasy® Mini Kit (Qiagen), using the protocol from the RNeasy® Mini Handbook (Qiagen). Cells were homogenised in 350 µl Buffer RLT containing 1% β-Mercaptoethanol (Sigma-Aldrich). Homogenised cells were passed through a 20-gauge needle, attached to a ribonuclease (RNase)-free syringe, 15 times. One volume of 70% ethanol was added to the homogenised lysate and aspirated. Seven-hundred microlitres of lysate was transferred to an RNeasy® column and centrifuged for 15 seconds at 8000 x g. Following centrifugation the flow-through was discarded, and the process was repeated until all of the lysate was passed through the column. All flow-through was always discarded, unless specified otherwise. Three-hundred-and-fifty microlitres of RW1 solution was added to the column and centrifuged for 15 seconds at 8000 x g. Eighty microlitres of deoxyribonuclease (DNase) 1 incubation mix was pipetted directly onto the spin column membrane, and allowed to incubate at room temperature for 15 minutes. Following incubation, 350 µl of RW1 solution was added

to the spin column, and centrifuged for 15 seconds at 8000 x g. Subsequently, 500 µl Buffer RPE solution was pipetted onto the spin column and centrifuged for 15 seconds at 8000 x g. An additional 500 µl of Buffer RPE solution was pipetted on to the spin column and centrifuged for 2 minutes at 8000 x g. The RNeasy® spin column was centrifuged at 10000 x g and transferred to a new 1.5 ml collection tube, to ensure that no Buffer RPE solution was transferred to the new collection tube. Fifty microlitres of nuclease-free water was pipetted onto the spin column and centrifuged for 1 minute at 8000 x g. The flow-through in the collection tube was pipetted onto the spin column and centrifuged for 1 minute at 8000 x g. The RNA yield was established using the NanoDrop™ technology, and samples were stored at -80°C.

2.8. RNA precipitation

In order to increase the working concentration of RNA, by reducing the total volume of diluent from 50 µl to 10µl, alcohol precipitation was done. The protocol used for ethanol precipitation was adapted from Zumbo, (n.d.). Extracted RNA was allowed to thaw on ice. Once thawed, 7.5 µl of 2 M sodium acetate, and 1 µl of 20 mg/ml glycogen was added to each sample and mixed gently. Once mixed, 58 µl isopropanol was added to each sample, mixed gently, and allowed to incubate overnight at -20°C. After incubation, samples were centrifuged at 4°C for 30 minutes at 12000 x g. The supernatant was discarded, whereas the pellet remained fixed to the centrifuge tube. The RNA pellet was resuspended in 110 µl of 75% ethanol, and centrifuged at 4°C for 15 minutes at 12000 x g. Samples were incubated at room temperature for 15 minutes, to ensure co-precipitated salts were dissolved. Once incubation had occurred, samples were centrifuged at 4°C for 5 minutes at 12000 x g. The supernatant was discarded, and the pellet was not disturbed. The 75% ethanol rinse step, and all subsequent steps were repeated. RNA pellets were left to dry for 15 minutes at 37°C on a dry heat block. Once dry, the RNA pellets were resuspended in 10 µl of nuclease-free water, and incubated for 15 minutes at room temperature to ensure complete RNA solubilisation.

2.9. Complementary deoxyribonucleic acid (cDNA) synthesis

Synthesis of cDNA for all samples was done using the High-Capacity cDNA Reverse Transcription Kit (Applied Biosystems), according to kit specifications. The kit components which were used to create the master mix were thawed on ice. A sufficient volume, for 65 reactions, of master mix was prepared for all samples (60). The master mix contained 130 µl 10x reverse transcriptase (RT) buffer, 52 µl 25x 100 mM deoxynucleotide (dNTP) mix, 130 µl

10x RT random primers, 65 µl Multiscribe™ reverse transcriptase, and 273 µl nuclease-free water (H_2O), mixed together to produce a total volume of 650 µl. Master mix (10 µl) was added to each sample, which contained the full volume of RNA (10µl), and mixed gently. Reverse transcription was performed using a thermal cycler using the following settings: 25°C for 10 minutes, 37°C for 120 minutes and 85°C for 5 minutes. Following cDNA synthesis, samples were stored at -20°C until required for Real-Time qRT-PCR.

2.10. Primer design

Primers were designed using the Integrated DNA Technologies PrimerQuest© online tool. Primers were designed for *TGF-β_1*, *TGF-β_2*, *TGF-β_3*, *ESR-α*, *ESR-β*, *PGR* and *VEGF A*. mRNA sequences were obtained from the National Center for Biotechnology Information (NCBI) Reference Sequence Database (RefSeq) database. Sequences were run through Basic Local Alignment Search Tool (BLAST) search to ensure that there were no similarities in sequences. In the case of transcript variants, the transcript variant with the largest mRNA sequence was downloaded. This sequence was analysed against all the known transcript variants using the sequence alignment BLAST search. Once the sequence alignment was established, the aligned sequence present in all transcript variants of the gene was analysed using a BLAST search. A sequence was considered specific for a gene when the BLAST search acquired similarity to only the transcript variants of the gene of interest. Primers were only designed for the sequence that was specific to the gene of interest. PrimerQuest© (Integrated DNA Technologies) was used for all primer design and primer parameters were set to specific Real-Time qRT-PCR standards. The most viable primers were chosen according to their sequence length, melting temperature and GC content (%) from the list of possible primers provided.

2.11. Real-Time Quantitative Reverse Transcription PCR (Real-Time qRT-PCR)

The samples used for Real-Time qRT-PCR were thawed on ice prior to plating, and a separate plate was used for each gene that was measured. Sample cDNA was diluted in a 1:1 ratio with nuclease-free water prior to use. cDNA from a metastatic ovarian cell line (provided by Prof. Raquel Duarte) was used as a positive control, at a working concentration of 7.5 ng/µl, diluted in nuclease-free water. Each plate contained all of the samples, and both the positive control as well as a no template control (NTC) containing the master mix specific to the gene of interest. Each well contained 7.5 µl of master mix, composed of 2.1 µl nuclease-free water, 0.2 µl forward primer (Integrated DNA Technologies), 0.2 µl reverse primer (Integrated DNA

Technologies) and 5 µl PowerUp™ SYBR™ Green Master Mix (Applied Biosystems). Each sample well contained 2.5 µl cDNA from the gene of interest, the positive control wells contained 2.5 µl cDNA from the control sample, and the NTC contained 2.5 µl nuclease-free water. Prior to Real-Time qRT-PCR analysis, plates were sealed and centrifuged at 300 x g for 1 minute. Real-Time qRT-PCR was run on 96-well plates using the PikoReal™ Real-Time PCR System (Thermo Fisher Scientific). The cycling conditions specified for PowerUp™ SYBR™ Green Master Mix (Applied Biosystems) were used: Uracil-DNA-glycosylase (UDG) activation at 50°C for 2 minutes, Dual-Lock™ DNA polymerase at 95°C for 2 minutes, denature at 95°C for 15 seconds and anneal at 60°C for 1 minute (50 cycles). A melt curve was established during the Real-Time qRT-PCR run using the following conditions: 95°C for 15 seconds (ramp rate of 1.6°C/second), 60°C for 1 minute (ramp rate of 1.6°C/second) and 95°C for 15 seconds (ramp rate of 0.15°C/second).

The quantitation cycle (Cq) values and the melt curve for each sample was acquired using PikoReal™ Software Version 2.2 (Thermo Fisher Scientific). Real-Time qRT-PCR runs were considered valid if the positive control expressed a Cq value and the NTC did not. Analysis of the measured genes was conducted by calculating the normalised relative quantification (NRQ) of a gene to the two reference genes, *Ubiquitin C* (*UBC*) and *tyrosine 3-monooxygenase/tryptophan 5-monooxygenase activation protein zeta* (*YWHAZ*) using the data obtained with the relative fold gene expression formula:

$$\text{fold gene expression} = 2^{-\Delta\Delta Cq}$$

2.12. Enzyme-linked immunosorbent assay (ELISA)

DuoSet® ELISAs (R&D Systems) were performed for *VEGF* (DY293B**)** and *IL-6* (DY06) on the culture media of the hormonally stimulated cells (Section 2.6.), as per the manufacturer's instructions. The 96-well microplates were incubated at room temperature overnight using 100 µl of 1 µg/ml capture antibody for *VEGF A* and 2 µg/ml capture antibody for *IL-6*. The microplates were then washed by pipetting 400 µl of wash buffer into each well, and aspirating the contents out. The wash step was performed three times. Blocking was initiated by the addition of 300 µl of reagent diluent, containing 10% bovine serum albumin (BSA) solution, into each well, and samples were incubated for 1 hour at room temperature to ensure complete blocking. A triplicate wash step was then conducted using wash buffer. Standards were prepared through seven serial dilutions. *VEGF* was diluted from 2000 pg/ml to 31.3 pg/ml and *IL-6* was diluted from 600 pg/ml to 9.38 pg/ml. One-hundred microlitres of each sample,

standard or positive control was added into individual wells and incubated for 2 hours at room temperature. Wells were subsequently washed in triplicate using 400 µl of wash buffer. Each well was incubated with 100 µl of 100 ng/ml detection antibody for *VEGF A* and 50 ng/ml detection antibody for *IL-6* for 2 hours at room temperature. A triplicate wash step was performed using 400 µl of wash buffer. A 40-fold dilution of Streptavidin-horseradish peroxidase (-HRP) (100 µl) was added to each well and incubated in the dark at room temperature for 20 minutes. Four-hundred microlitres of wash buffer was added to each well in triplicate after incubation. Once washed, 100 µl of substrate solution was added to each well, and the plate was incubated in the dark at room temperature for 20 minutes. Fifty microlitres of stop solution was added to each well and mixed thoroughly. The optical density of each sample was analysed using a wavelength of 450 nm. The experiment was considered successful if the following criteria were met: a standard curve could be constructed; the blanks did not express, and the positive controls showed expression. Results were analysed and a five-parameter logistic curve for the standards was established using the online tool obtained from https://www.myassays.com.

2.13. Statistical analysis

The Spearman's rank correlation coefficient formula was used to determine the correlation of live mean cell percentage (Section 2.5) with the percentage of genes expressed (Section 2.11):

$$\rho = 1 - \frac{6 \sum d_i^2}{n(n^2 - 1)} \qquad (1)$$

ρ is the Pearson correlation coefficient, d_i is the difference between the two ranks of each observation and n is the number of observations.

Additionally, another Spearman rank correlation coefficient was established to measure whether the total live cell count correlated with the total percentage of genes expressed. If samples expressed the same rank a correction factor was added to the Spearman rank correlation coefficient formula:

$$\mathrm{CF} = \frac{m\,(m^2 - 1)}{12} \qquad (2)$$

CF is the correction factor and m is the number of times an item or rank is repeated.

Combining equation 1 and equation 2 gives:

$$\rho = 1 - \frac{6 \sum d_i^2 + \mathrm{CF}}{n(n^2 - 1)} \qquad (3)$$

ρ is the Pearson correlation coefficient, d_i is the difference between the two ranks of each observation, CF is the correction factor and n is the number of observations.

Chapter 3: Results

3.1. Human endometrial stromal cells (HESCs)

26 samples of endometrial biopsies were obtained from healthy, reproductively active women undergoing D&C, following informed consent. Of these 26 samples, only 5 were successfully isolated.

3.1.1. Predisposition to microbial infection

Endometrial samples showed a predisposition to microbial infection, and increasing the concentration of antimicrobial agents in solution improved cell yield.

The biopsied tissue collected and used for the isolation of HESCs were observed to exhibit a predisposition to bacterial and fungal infection prior to initiation of stromal cell isolation. The initial transport media (RPMI–1640 with L-glutamine (Lonza), 5% FCS and 0.1% Penicillin-Streptomycin-Amphotericin 100X (Lonza)) showed inadequate efficacy in limiting bacterial or fungal infection post-collection. Increasing the concentration of Penicillin-Streptomycin-Amphotericin 100X (Lonza) from a 0.1% to a 0.2% solution within the transport media displayed positive results and decreased the observed levels of infection post-isolation.

3.1.2. Presence of blood during isolation procedure

Blood exhibited deleterious effects on HESC isolation. The removal of blood and its subsequent coagulation improved cell yields through isolation.

Collected tissue samples were intensely haematic post-collection. The blood contained within the tissue biopsies affected the isolation of stromal cells, particularly during the tissue mincing and collagenase digestion stages of isolation. The blood present within the tissue biopsy was removed by the immersion of samples in PBS, pH 7.4, prior to both the tissue mincing and collagenase procedures. The washing steps visibly reduced the quantity of blood present within the endometrial biopsies, which in turn decreased the coagulation normally associated with tissue mincing. The addition of extra washing steps improved the amount of viable tissue which could be minced, and increased the yield of cells post-isolation.

Minced tissue expressed a propensity towards aggregation during collagenase incubation. This was observed as the aggregation of minced tissue decreased the effectiveness of collagenase in breaking cellular bonds. Additional PBS rinse steps were added, prior to incubation with

collagenase, to alleviate tissue clumping. Furthermore, the tissue was vortexed every 10 minutes during incubation. Additional wash steps in conjunction with cyclical vortexing decreased the levels of tissue aggregation, which improved the overall yield of isolated cells.

3.1.3. Morphology *in vitro*

3.1.3.1. Morphology after 24 – 48 hours

Initial cellular attachment occurred 24 – 48 hours post-isolation. Stromal cells were more numerous than epithelial cells.

The procedure used for the isolation of HESCs yielded cells post-isolation. Isolated cells exhibited initial attachment to culture flasks 24 - 48 hours after isolation. The majority of cells did not exhibit specific morphology under light microscopy, and appeared small and circular (Figure 2). Regions of growth appeared, with small clusters of cells forming in multiple regions throughout the culture flask (Figure 2). There were two distinct cell types present 24 – 48 hours post-isolation: HESCs and epithelial cells. HESCs appeared more numerous and formed larger colonies than epithelial cells 24 – 48 hours post-isolation (Figure 2). HESCs appeared long and spindle-like with cytoplasmic projections extending throughout the culture flask. These cells exhibited clearly defined cytoplasmic borders and had visible nucleoli, and were also the larger of the two cell types observed (Figure 2). Epithelial cells appeared smaller and established smaller clusters of cells. The growth of these cells occurred as a whorl-like formation (Figure 2).

3.1.3.2. Morphology after 72 – 96 hours

HESCs exhibited greater distribution throughout the flask and displayed varying morphologies 72 – 96 hours post isolation.

Larger cell colonies appeared 72 - 96 hours post-isolation and fewer small isolated cells were present (Figure 3). Again, HESCs were more numerous and exhibited greater distribution throughout the culture flask compared to epithelial cells (Figure 3). HESCs established larger colonies than those exhibited by epithelial cells. Additionally, HESCs on the periphery of the colony exhibited typical stromal cell morphology: large spindle-like cells with long cytoplasmic projections and clearly defined borders (Figure 3). The cells towards the centre of the colonies displayed a polygonal morphology with fewer visible cytoplasmic projections; however, cells still displayed clearly defined borders (Figure 3).



Figure 2: Cell colonies from human endometrial samples present in vitro 48 hours post-isolation

The white arrow indicates the stromal cell colony. The black arrow indicates the epithelial cell colony. The yellow arrow indicates the cells with no particular morphology. X40 magnification.

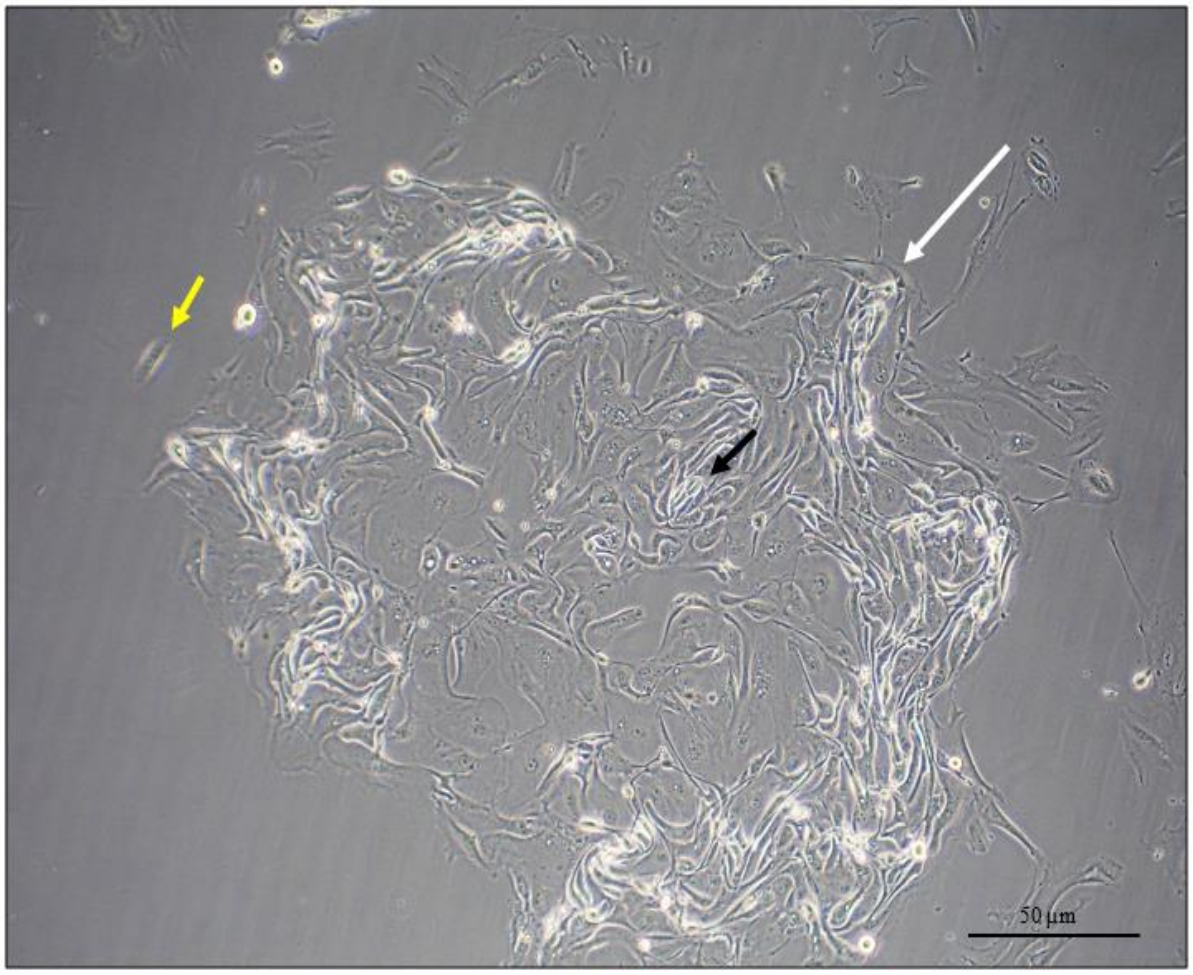


Figure 3: Cell colonies from human endometrial samples present in vitro 72 hours post-isolation

The white arrow indicates the entire stromal cell colony. The black arrow indicates the centre of the colonies, which exhibit a polygonal morphology with fewer visible cytoplasmic projections. The yellow arrow indicates cells with no particular morphology. X40 magnification.

3.1.3.3. Confluency after 192 – 240 hours

Confluent HESCs displayed polygonal morphology and clearly defined borders.

Confluency was reached after 192 – 240 hours (8 – 10 days) in primary culture. Colonies of cells were no longer visible, and there was very limited space between cells (Figure 4). Cells did not exhibit any specific arrangement and cytoplasmic projections appeared to extend in multiple directions throughout the flask. Stromal cells exhibited a polygonal morphology and were stacked closely together. However, the morphology was difficult to establish due to the presence of the cytoplasmic projections (Figure 4). Cells exhibited clearly defined cytoplasmic borders and appeared to overlap other cells and cytoplasmic projections (Figure 4). The appearance of clearly visible nuclei was limited due to the overlapping of cells; however, when the nuclei were visible, they appeared large and round with prominent nucleoli (Figure 4)

3.2. Human endometrial stromal cell (HESC) viability

3.2.1. Post-cryopreservation

Cells exhibited impaired attachment and poor viability after being stored at -80 °C.

Cell samples stored at -80 °C (see section 2.4.) showed impaired function during passaging following the isolation and initial passaging procedures. Cells displayed impaired attachment capabilities to culture-appropriate plastic ware.

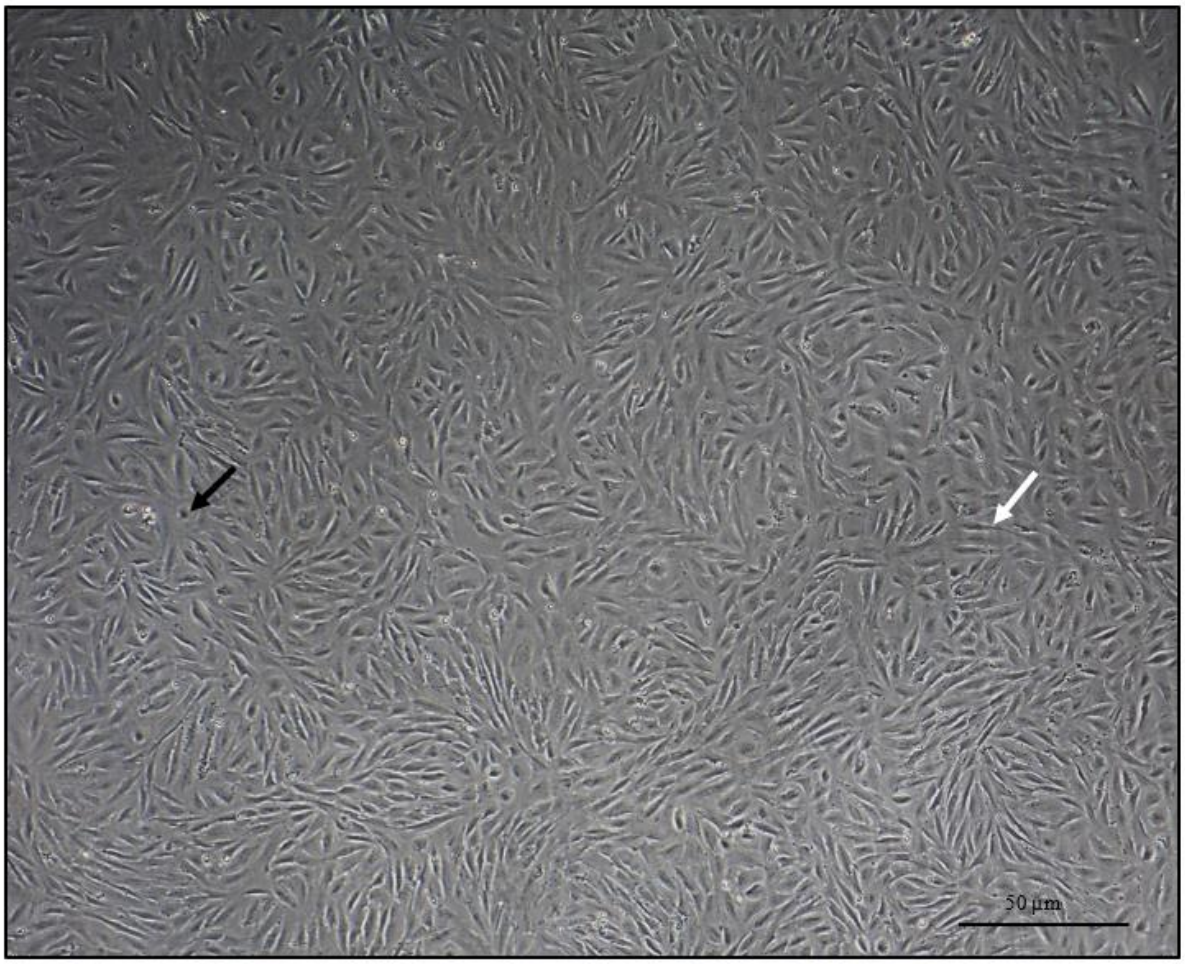


Figure 4: Cell colonies from human endometrial samples present in vitro 240 hours post-isolation

The white arrow indicates the clearly defined cytoplasmic border. The black arrow indicates the large, round nuclei with prominent nucleoli. X40 magnification.

3.2.2. Troubleshooting

Troubleshooting proved unsuccessful in improving cell viability.

Troubleshooting aimed to improve the growth and attachment rates of cells; however, all methods proved to be unsuccessful. Initial troubleshooting methods aimed at ensuring that the cells were adequately washed prior to incubation. Additional washing steps ensured the total removal of DMSO; however, cells continued to show insignificant growth and attachment. Culture flasks were replaced with flasks of known efficacy. The alteration of culture plastic-ware displayed negligible improvement to the survivability of cells. All culture media and constituents of growth media (FCS and Penicillin-Streptomycin-Amphotericin) were replaced with ones of known efficacy. However, these alterations did not improve the viability of cells. Multiple incubators were used; however, low cell viability remained unchanged. Troubleshooting was halted due to a finite amount of sample. Due to the inability to culture more cells *in vitro*, it was decided to retain remaining sample stock, to ensure progression of the research.

When samples were required, two cryovials were removed from the freezer, washed with PBS, pH 7.4, and left to grow at 37°C for 24 hours in growth media (RPMI 1640 with L- glutamine, 10% FCS and 0.1% Penicillin-Streptomycin-Amphotericin 100X (Lonza)). All cell samples were counted in duplicate using a TC20 automatic cell counter (Bio-Rad) with trypan blue (0.4%) counterstain post-incubation.

3.2.3. Viability counts

Cell counts were low in each patient sample (Figure 5 & Table 1). Mean total populations (Figure 5) for individual samples were all below 3×10^5 cells. Patient 1 had the highest cell count, whereas Patient 3 had the lowest cell count. No mean live cell count exceeded 5×10^4 cells (Figure 5), and all mean live cell percentages were below 20%. Patient 5 had the highest live cell percentage, whereas Patient 4 had the lowest live cell percentage (Table 1).

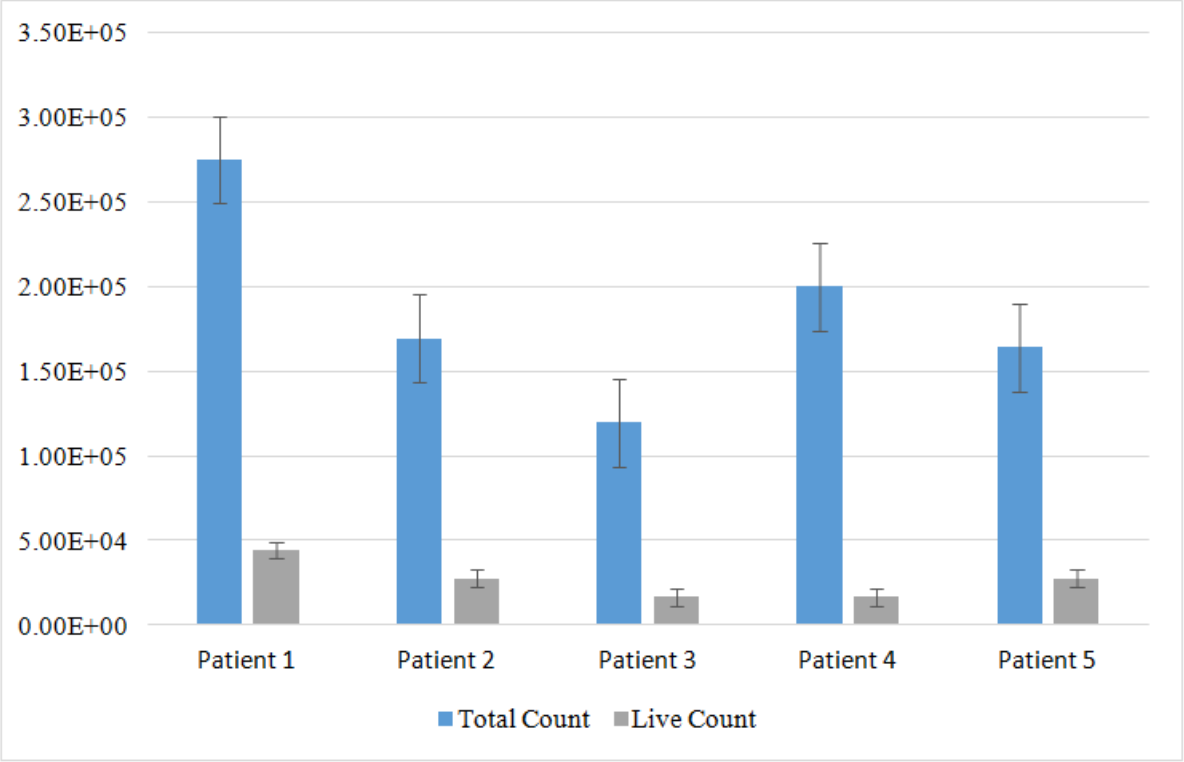


Figure 5: Mean cell counts of patients

The mean total count (■) and the live count (■) of patients 1-5 were calculated in 1 µl of solution.

	Patient 1	Patient 2	Patient 3	Patient 4	Patient 5
Mean Live Cells (%)	**16.15%**	**16.37%**	**13.95%**	**8.34%**	**16.92%**

Table 1: Mean percentage of living cells in Patients 1 – 5

3.2.3.1. Patient 1

Patient 1 displayed the highest mean total cell count and mean living cell count.

Patient 1 displayed both the highest mean total cell count (2.75×10^5) and mean living cell count (4.44×10^4) (Figure 5). Cells were counted and separated according to diameter (Figure 6). Dead cells were more numerous than living cells at all diameters (Figure 6). Cell diameter ranged from 5 µm to 16 µm, with the highest populations seen in the ranges 5 µm to 7 µm and 9 µm to 11 µm. The dead cells exceeded living cells by 7-fold in the 5 µm to 7 µm range and by 5-fold in the 9 µm to 11 µm range.

3.2.3.2. Patient 2

Patient 2 had a mean total cell count of 1.70×10^5 and a mean living cell count of 2.78×10^4 (Figure 5). Individual cell counts for Patient 2 were separated according to diameter (Figure 7). Dead cells were more numerous than living cells at all diameters (Figure 7). Cell diameter ranged from 5 µm to 19 µm with the highest populations seen in the ranges 5 µm to 6 µm and 10 µm to 13 µm. The dead cells exceeded living cells by 10-fold in the 5 µm to 6 µm range and by 2-fold in the 10 µm to 13 µm range.

3.2.3.3. Patient 3

Patient 3 displayed the lowest mean total cell count and joint lowest mean living cell count.

Patient 3 exhibited the lowest mean total cell count of all five samples (1.20×10^5) and the joint lowest mean living cell count (1.67 x 104) (Figure 5). The mean percentage of living cells was second lowest out of all five patient samples (Table 1). Cell counts for Patient 3 were separated according to diameter (Figure 8). Dead cells were more numerous than living cells at all diameters (Figure 8). Cell diameter ranged from 5 µm to 17 µm with the highest populations seen in the ranges 5 µm to 7 µm and 12 µm to 14 µm. The dead cells exceeded living cells by 7-fold in the 5 µm to 7 µm range and by 3-fold in the 12 µm to 14 µm range.

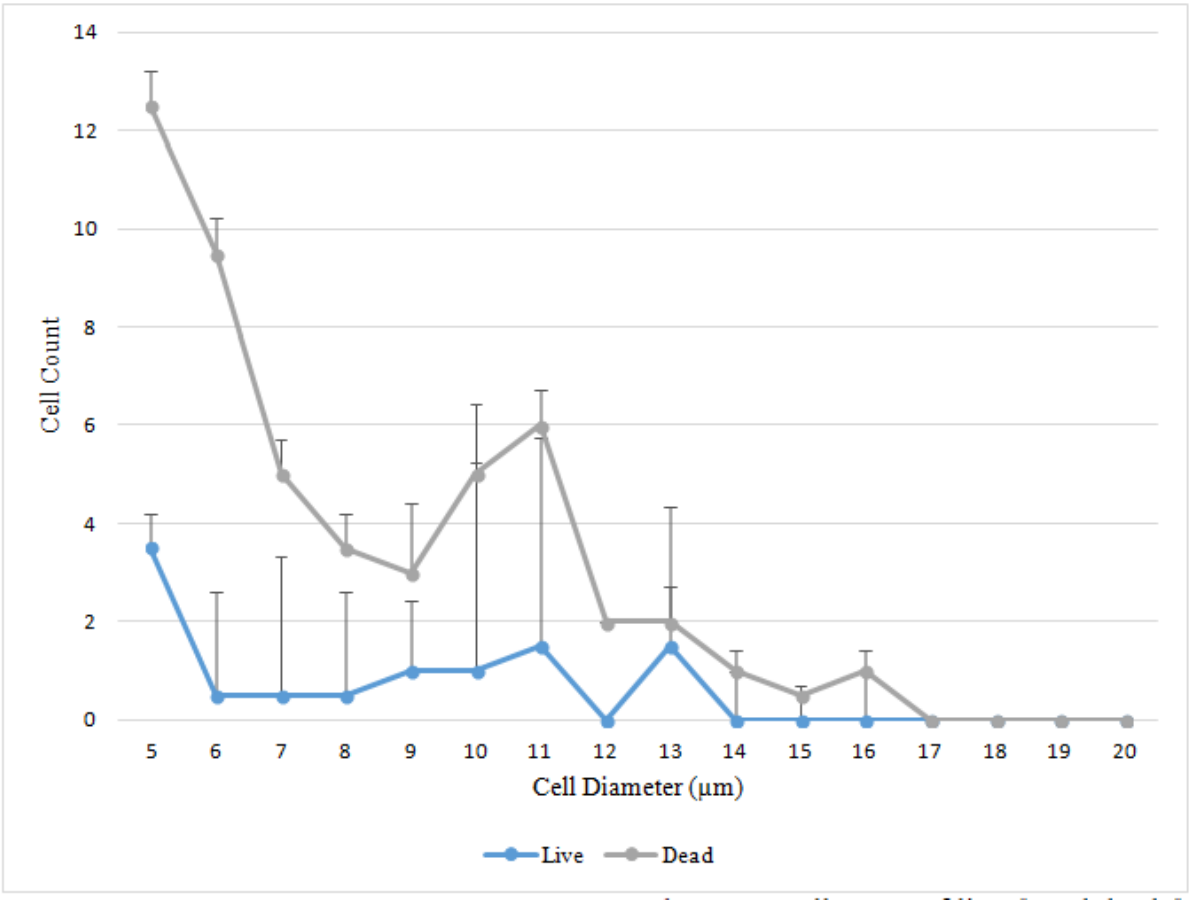


Figure 6: Individual cell counts for patient 1

The mean cell count of live (●) and dead (●) cells for patient 1 in 10 µl of solution are shown according to diameter.

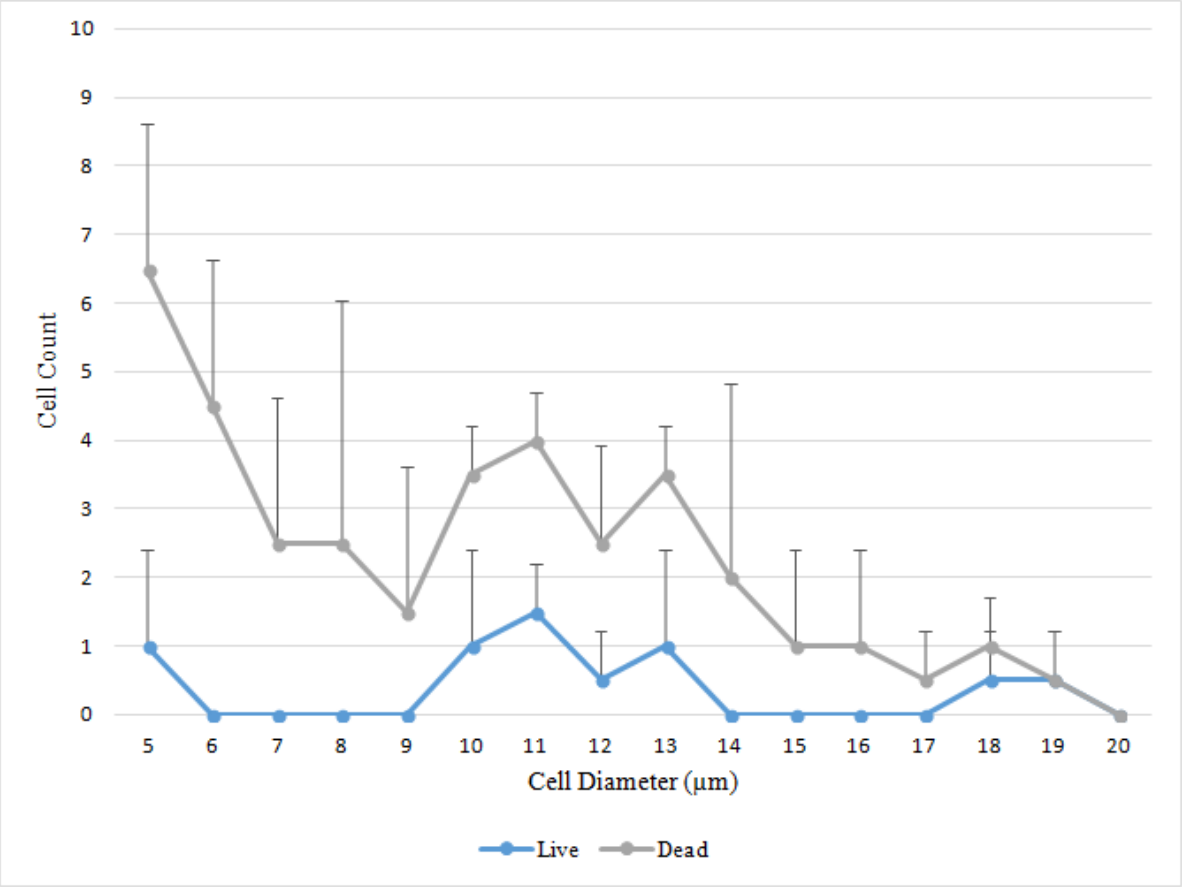


Figure 7: Individual cell counts for patient 2

The mean cell count of live (●) and dead (●) cells for patient 2 in 10 µl of solution are shown according to diameter.

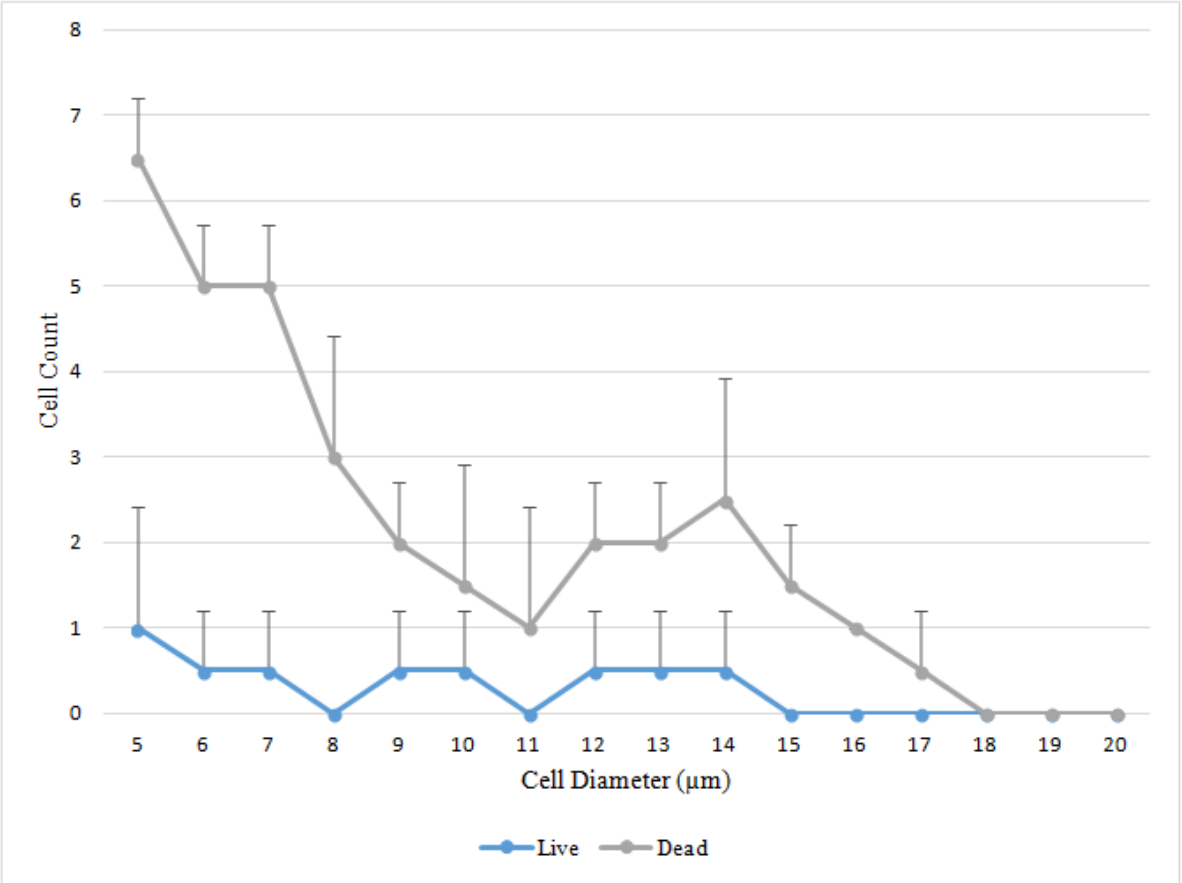


Figure 8: Individual cell counts for patient 3

The mean cell count of live (●) and dead (●) cells for patient 3 in 10 µl of solution are shown according to diameter.

3.2.3.4. Patient 4

Patient 4 displayed the second highest mean total cell count and joint lowest mean living cell count.

Patient 4 displayed the second highest mean total cell count (2.00×10^5) and the joint lowest mean living cell count (1.67×10^4) (Figure 5). Therefore, the mean percentage of living cells was the lowest out of all five patient samples at for Patient 4 (Table 1). Cell counts for Patient 4 were separated according to diameter (Figure 9). Dead cells were more numerous than living cells at all diameters (Figure 9). Cell diameter ranged from 5 µm to 18 µm. The highest populations of cells were seen in the range of 5 µm to 9 µm, and dead cells exceeded living cells by 13-fold.

3.2.3.5. Patient 5

Patient 5 exhibited the highest mean percentage of living cells.

Patient 5 had a mean total cell count of 1.64×10^5 and a mean living cell count of 2.78×10^4 (Figure 5). The mean percentage of living cells for Patient 5 was the highest of all 5 patient samples at (Table 1). Cell counts for Patient 5 were separated according to diameter (Figure 10). Dead cells were more numerous than living cells at all diameters (Figure 10). Cell diameter ranged from 5 µm to 17 µm with the highest populations seen in the ranges 5 µm to 8 µm and 11 µm to 14 µm. The dead cells exceeded living cells by 6-fold in the 5 µm to 8 µm range and by 4-fold in the 11 µm to 14 µm range.

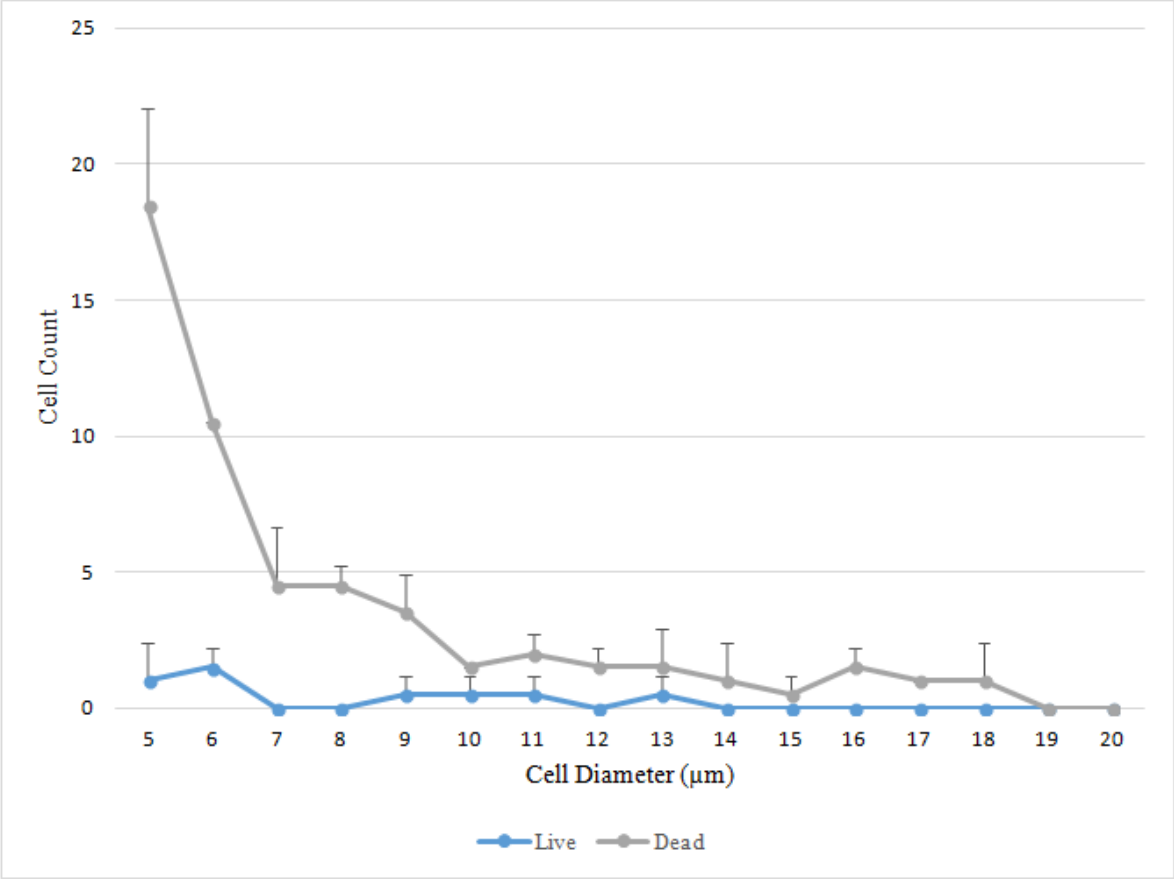


Figure 9: Individual cell counts for patient 4

The mean cell count of live (●) and dead (●) cells for patient 4 in 10 µl of solution are shown according to diameter.

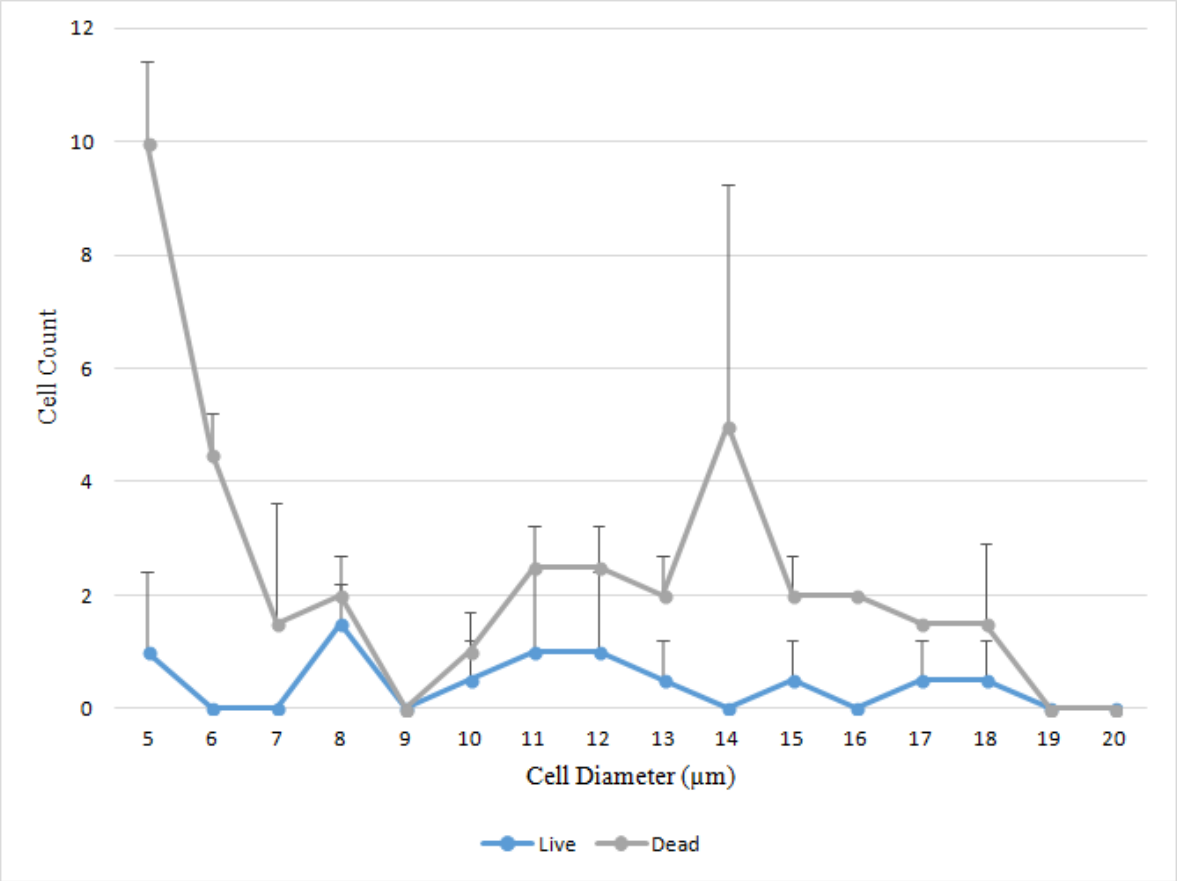


Figure 10: Individual cell counts for patient 5

The mean cell count of live (●) and dead (●) cells for patient 5 in 10 µl of solution are shown according to diameter.

3.3. Real-Time Quantitative Reverse Transcription PCR (Real-Time qRT-PCR) setup and analysis

3.3.1. Primer Design

Primers were designed for *TGF-β_1*, *TGF-β_2*, *TGF-β_3*, *ESR-α*, *ESR-β*, *PGR* and *VEGF A* according to the general procedure described in chapter 2.10. Table 2 indicates the primer pairs that were designed for each of the aforementioned genes. Each gene analysed has a varying amount of transcript variants. The details pertaining to the transcript variant design strategy per gene are available in Appendix B.

3.3.2. Primer Analysis

Four of the seven designed primers (*TGF-β_1*, *ESR-α*, *PGR* and *VEGF A*) were tested for efficacy using Real-Time qRT-PCR. The genes were measured using a control sample of known gene expression (protein free metastatic ovarian cell line). All tested primers expressed only the gene of interest (Figure 11 and Table 3).

3.3.3. RNA Isolation

RNA concentration determination for HESCs was attempted using the NanoDrop^{TM}. However, the results produced were inconclusive. RNA concentration levels were too low for accurate readings to be achieved.

3.3.4. RNA Precipitation

Patient samples were subjected to precipitation and the total volume of RNA was reduced from 50 µl to 10 µl, to increase the working concentration of RNA. In order to preserve the limited RNA, precipitation was verified through the use of the experimental runs of Real-Time qRT-PCR analysis.

Table 2: Designed primers for *TGF-β*1, *TGF-β*1, *TGF-β*1, *ESR-α*, *ESR-β*, *PGR* and *VEGF A*

Gene	Type	Sequence (5' - - 3')	Start	Length (bp)	Tm (ºC)	GC (%)	Amplicon (bp)
TGF-B₁	**Forward Primer**	CCTGCCTGTCTGCACTATTC	2 243	20	62.29	55	
	Reverse Primer	TGCCCAAGGTGCTCAATAAA	2 340	20	62.41	45	
	Product						98
TGF-B₂	**Forward Primer**	CGGAGGTGATTTCCATCTACAA	1 612	22	61.96	45.46	
	Reverse Primer	AAGGGCGGCATGTCTATTT	1 750	19	61.93	47.37	
	Product						139
TGF-B₃	**Forward Primer**	GAGAGTCAAGTCCAAGGGAATG	119	22	62.23	50	
	Reverse Primer	CTGCTCCGGAAAGCTGTTAT	204	20	62.19	50	
	Product						86
ESR-α	**Forward Primer**	GCTTCGATGATGGGCTTACT	568	20	61.99	50	
	Reverse Primer	CCTGATCATGGAGGGTCAAATC	678	22	62.43	50	
	Product						109
ESR-β	**Forward Primer**	GATCGCTAGAACACACCTTACC	422	22	62.17	50	
	Reverse Primer	AGTGAGCATCCCTCTTTGAAC	532	21	62.16	47.62	
	Product						111
PGR	**Forward Primer**	ATTACCAGTGTTCCCGTCTTC	7 436	21	61.85	47.62	
	Reverse Primer	CCTGTACTTCCTCCAGCATAAG	7 546	22	61.80	50	
	Product						111
VEGF A	**Forward Primer**	TGGTGTCTTCACTGGATGTATTT	2195	23	62	39.1	
	Reverse Primer	AGTCTCTCATCTCCTCCTCTTC	2272	22	62	50	
	Product						99

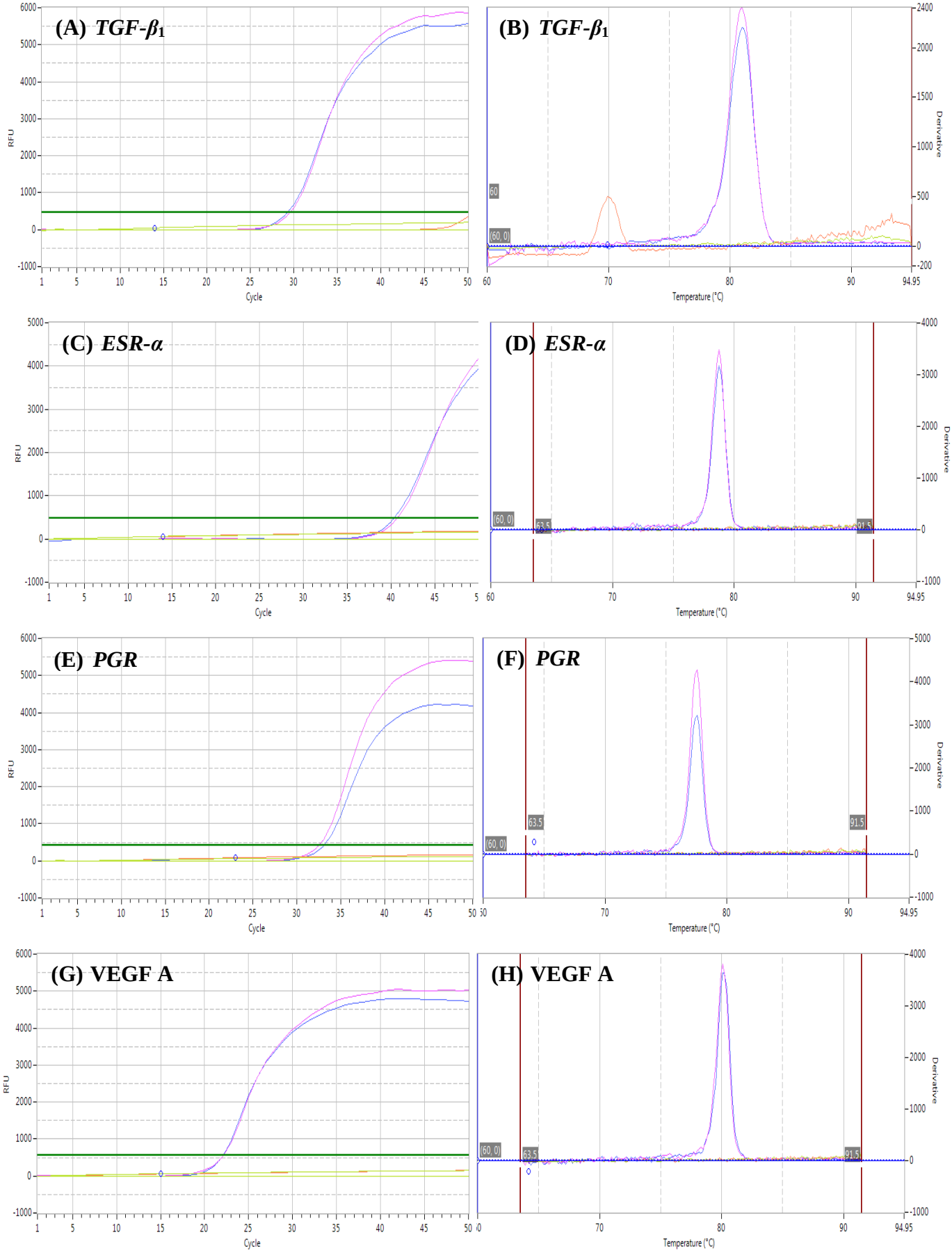


Figure 11: Primer efficacy Cq values of (A) *TGF-β*$_1$, (C) *ESR-α*, (E) *PGR* and (G) *VEGF A* and the Melting Temperatures of (B) *TGF-β*$_1$, (D) *ESR-α*, (F) *PGR* and (H) *VEGF A*.

Table 3: Cq and melting temperature of analysed genes

	Mean Cq	SD of Cq (σ)	Mean Melting Temperature (°C)	SD of Melting Temperature (σ)
***TGF-β*$_1$**	29.44	0.20	80.93	0.03
ESR-α	40.47	0.24	78.75	0.03
PGR	32.76	0.42	77.49	0.00
VEGF A	22.09	0.02	80.13	0.05

3.3.5. Real-Time Quantitative Reverse Transcription PCR (Real-Time qRT-PCR) Analysis

The Real-Time qRT-PCR results showed very little statistical significance, as a result of the low RNA yield. However, the results obtained from the specific genes that were analysed show possible trends.

3.3.5.1. Reference Genes

HESC samples contained low levels of initial RNA in comparison to the positive control sample.

RNA isolation and precipitation using HESCs was verified through the amplification of reference genes. Samples were run in duplicate and the mean was calculated (Table 4). RNA from HESCs showed gene amplification for the reference genes *UBC* and *YWHAZ*. Melting temperatures for *UBC* were similar between HESC and Protein Free samples (Table 4). The Cq values for the HESC samples were higher than that of the Protein Free sample (Table 4). The Cq values for the HESC ranged from 33.80 to 42.44 cycles whereas the mean Cq value for the protein free sample was 18.72 (Table 4). Similar results were seen in *YWHAZ* gene expression. Melting temperatures were similar between HESCs and the positive control sample (Table 4). The Cq values of the HESCs and Protein Free sample were dissimilar (Table 4). These results suggest that while RNA was present, and that the same gene was being expressed in both the HESCs and Protein Free samples (similar melting temperature), RNA was more abundant within the Protein Free sample (lower Cq value).

3.3.5.2. Oestrogen receptor α (*ESR-α*)

ESR-α expression did not increase in the presence of MPA.

Only Patient 1 and Patient 2 showed any expression of *ESR-α*. In the Patient 1 sample, only the one biological replicate in the MPA treatment group and control group expressed *ESR-α*. Patient 2 only showed expression of the gene in one of the control biological replicates. There appeared to be relatively minimal differences between the relative expression levels of *ESR-α* between the Control (3.71) and MPA (3.95) group (Figure 12). When both groups were compared, ESR-α showed a 6% increased expression level within the MPA group (Figure 12).

Table 4: Mean Cq and Melting Temperatures for *UBC* and *YWHAZ* genes

Patient Number	Sample Name	Mean Cq *UBC*	Mean Melting Temperature *UBC* (°C)	Mean Cq *YWHAZ*	Mean Melting Temperature *YWHAZ* (°C)
Patient 1	E_2 1	35,52	83,19	36,04	78,92
	E_2 2	35,98	83,04	35,11	78,81
	MPA 1	36,09	83,04	36,02	78,82
	MPA 2	34,05	82,12	34,68	78,76
	Control 1	33,85	81,73	34,71	78,80
	Control 2	34,25	82,40	36,26	78,83
Patient 2	E_2 1	35,57	83,11	35,35	78,83
	E_2 1	35,55	82,96	35,76	78,75
	MPA 1	35,14	82,89	35,41	78,67
	MPA 2	35,43	82,90	35,18	78,72
	Control 1	37,33	82,89	35,79	78,71
	Control 2	38,01	82,86	35,43	78,66
Patient 3	E_2 1	36,05	83,03	35,20	78,82
	E_2 2	-	-	-	-
	MPA 1	-	-	37,32	78,71
	MPA 2	42,44	82,80	36,32	78,70
	Control 1	35,98	82,88	37,41	78,69
	Control 2	35,28	82,91	35,84	78,75
Patient 4	E_2 1	-	-	-	-
	E_2 2	-	-	-	-
	MPA 1	36,47	82,87	35,27	78,71
	MPA 2	37,26	82,83	36,84	78,69
	Control 1	-	-	-	-
	Control 2	36,33	82,85	36,90	78,77
Patient 5	E_2 1	35,03	83,08	35,47	78,84
	E_2 2	33,80	83,01	36,39	78,76
	MPA 1	34,02	82,96	35,81	78,73
	MPA 2	33,99	82,86	35,97	78,66
	Control 1	33,83	82,915	34,37	78,71
	Control 2	34,08	82,93	34,86	78,745
Positive Control	Protein Free	18,72	82,68	20,15	78,41

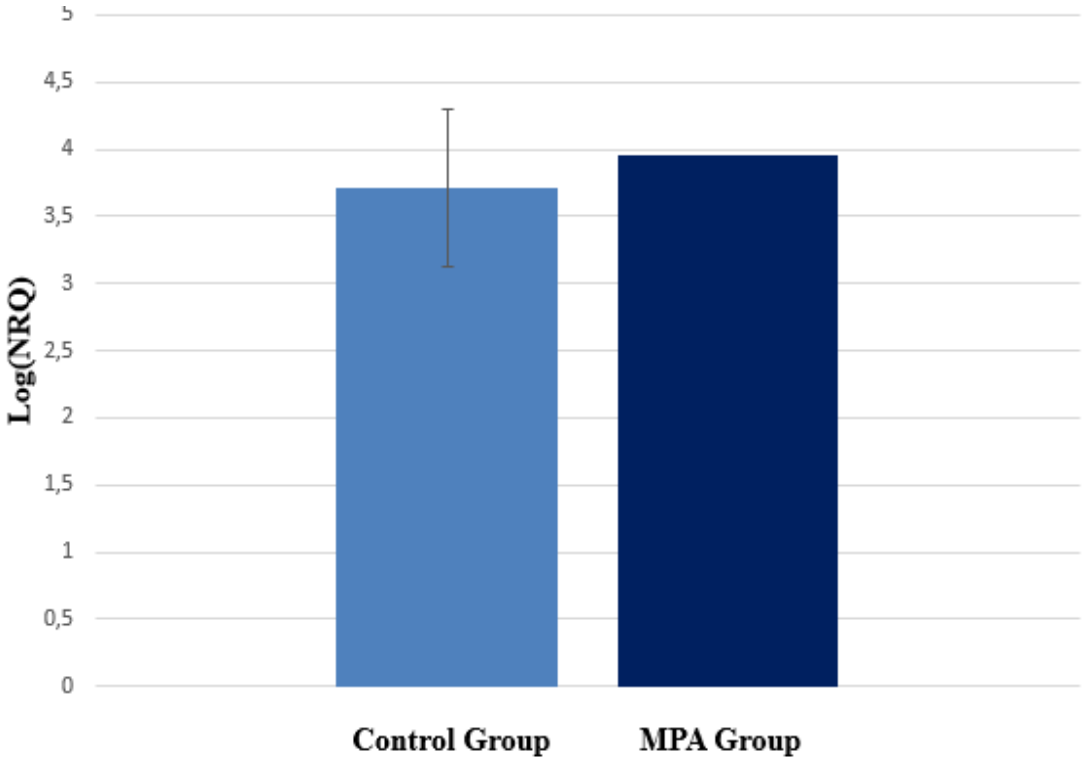


Figure 12: Normalised relative quantities of *ESR-α*

The mean log of the NRQ of samples from patients 1 and 2 is shown for *ESR-α* within the HESC groups

3.3.5.3. Progesterone receptor (*PGR*)

PGR exhibits minimal increased expression in the presence of E_2.

Patient 1 and Patient 5 produced gene expression in two of the three experimental groups. Both patients expressed the gene for the *PGR* in the E_2 treatment group, and in the control group. Patient 3 expressed the *PGR* gene in the E_2 treatment group. The *PGR* displayed minimal differences in relative gene expression within the E_2 treatment group (3.84) when compared to the expression levels of the control group (3.59) (Figure 13). When the two groups were compared, the control group expressed a decreased gene expression of *PGR* by 7%.

3.3.5.2. *Transforming growth factor β* (*TGF-β_1*)

TGF-β_1 expression is increased in the presence of E_2.

Patient 1 showed the highest propensity for gene expression. The E_2 biological replicates and one of the control group biological replicates expressed the gene *TGF-β_1*. Patient 3 showed expression in one of the E_2 biological replicates, and Patient 5 showed *TGF-β_1* expression in one of MPA biological replicates. The relative gene expression of *TGF-β*1 appeared to have higher expression levels of *TGF-β_1* within the E_2 treatment group when compared to the expression levels of both the MPA and control groups. In comparison with the control group, *TGF-β_1* presented a 35% increase when treated with E_2. *TGF-β_1* showed similar expression levels between the control and MPA groups with the control group expressing 4% more *TGF-β_1* than the MPA treatment group (Figure 14).

3.3.5.4. *Vascular endothelial growth factor* A (*VEGF A*)

VEGF A gene expression is increased when exposed to either E_2 or MPA.

Only Patient 1 and Patient 5 expressed the *VEGF A* gene. Patient 1 expressed *VEGF A* in both E_2 biological replicates, in both MPA biological replicates, and in one of the control biological replicates. Patient 5 expressed *VEGF A* in one E_2 biological replicate and in one MPA biological replicate, as well as in one control biological replicate group. The relative gene expression of *VEGF A* exhibited higher expression levels of *VEGF A* within the E_2 treatment group and the MPA treatment group, when compared to the expression levels within the control group (Figure 15). *VEGF A* showed a 20% increase in gene expression when treated with E_2, and a 19% increase when treated with MPA, when compared with the control group (Figure 15)

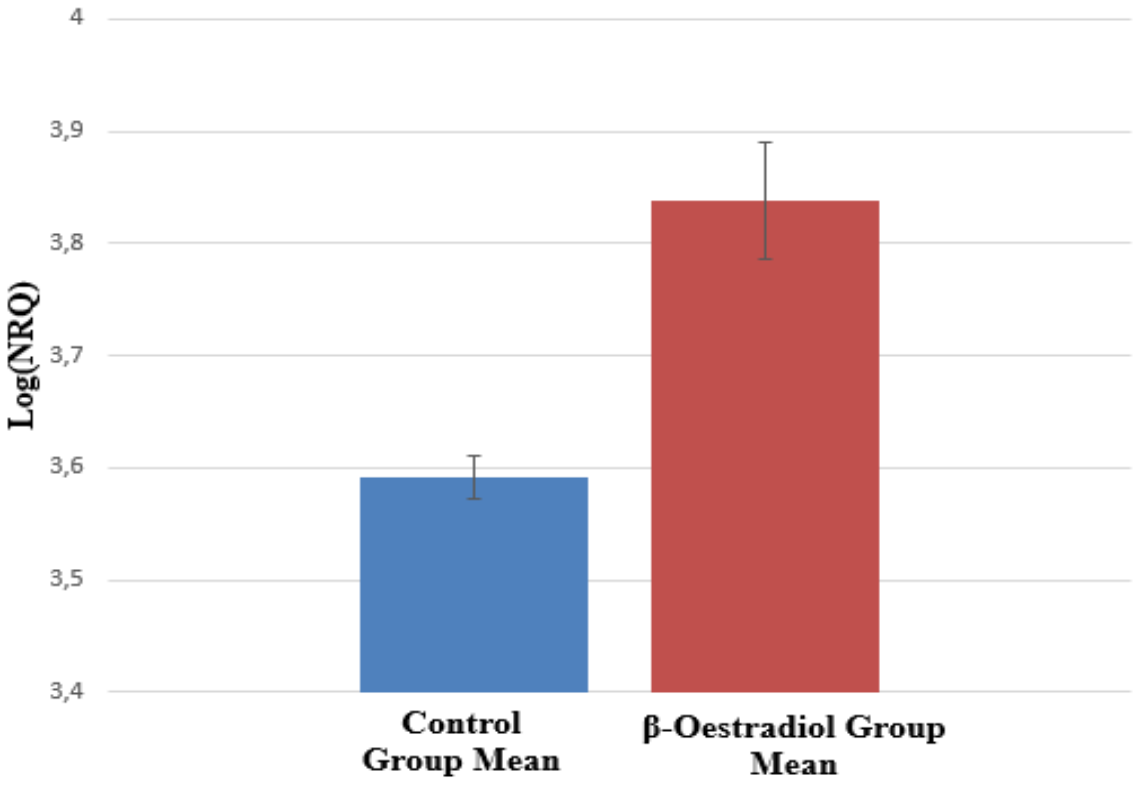


Figure 13: Normalised relative quantities of *PGR*

The mean log of the normalised relative quantities (NRQ) of samples from patients 1, 3 and 5 is shown for *PGR* within the HESC groups.

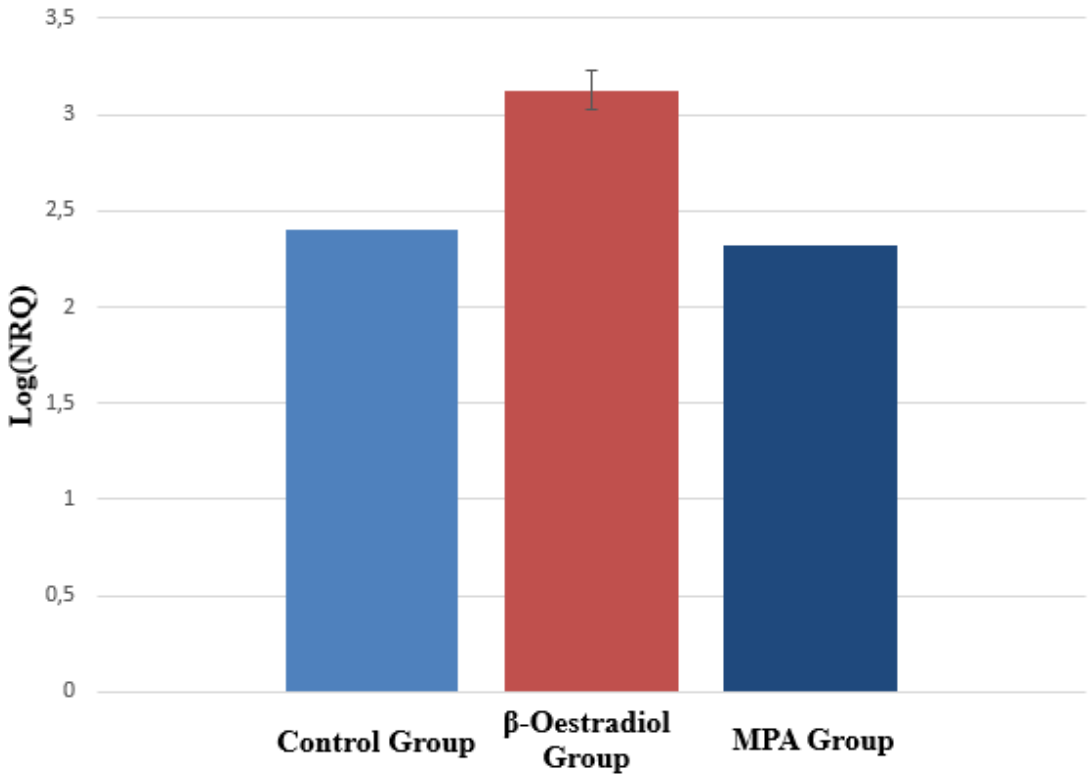


Figure 14: Normalised relative quantities of *TGF-β*1

The mean log of the normalised relative quantities (NRQ) of samples from patients 1, 3 and 5 is shown for *TGF-β_1* within the HESC groups.

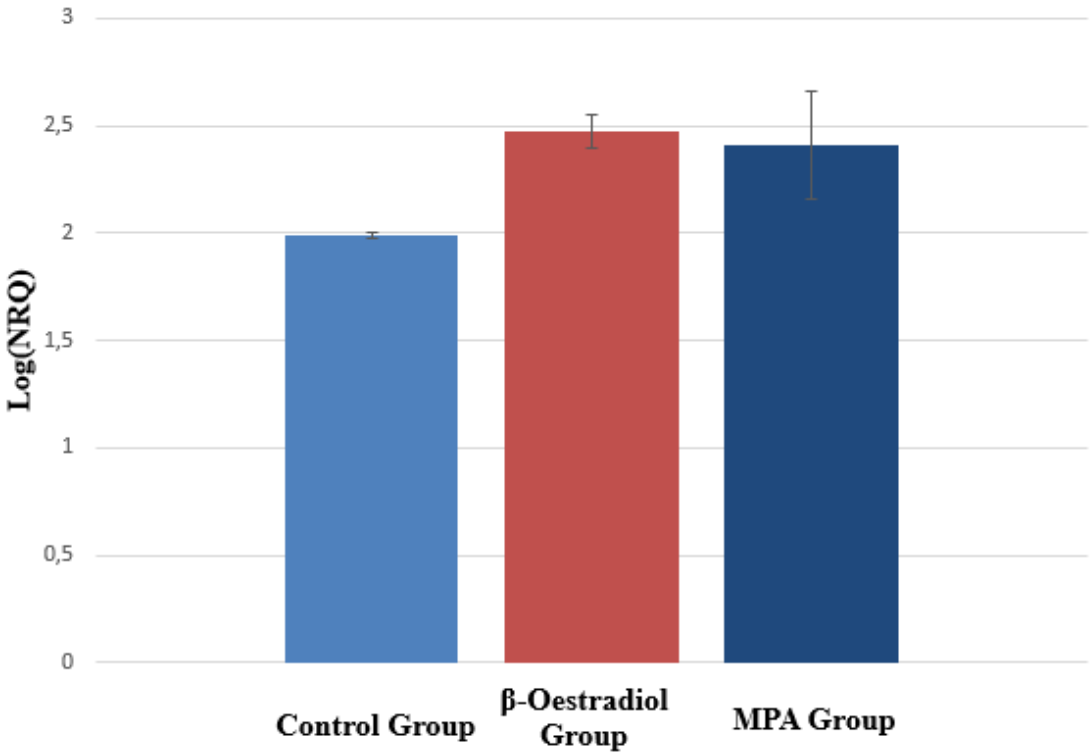


Figure 15: Normalised relative quantities of *VEGF A*

The mean log of the normalised relative quantities (NRQ) of samples from patients 1 and 5 is shown for *VEGF A* within the HESC groups.

3.4. Enzyme-linked immunosorbent assays (ELISAs)

3.4.1. *Interleukin-6* (*IL-6*)

The five-parameter logistic curve was used to measure the concentration of *IL-6* present within the supernatant of the samples and the control. Concentrations were established from the standards (Figure 16). A detectable concentration of *IL-6* was not expressed in the sample supernatant of any of the experimental groups. The three positive controls, when measured against the standard logistic curve, all expressed measurable concentrations of *IL-6*. Positive Control 1 showed the highest concentration of *IL-6* (7627 ng/ml), when compared to Positive Control 2 (404.40 ng/ml) and Positive Control 3 (10.44 ng/ml) (Figure 16).

3.4.2. *Vascular endothelial growth factor* A (*VEGF A*)

The five-parameter logistic curve was used to measure the concentration of *VEGF A* present within the supernatant of the samples and the control (Figure 17). No *VEGF A* was detected in the supernatants of samples in any of the experimental groups. The positive control, when measured against the standard logistic curve, expressed a measurable concentration of *VEGF* (21.77 ng/ml) (Figure 17).

3.5. Statistical Analysis

3.5.1. Real-Time Quantitative Reverse Transcription PCR gene expression

An in-depth statistical analysis of patient-derived Real-Time qRT-PCR results could not be conducted because all genes exhibited low levels of expression, with the exception of the reference genes (Table 4). The Real-Time qRT-PCR data show possible trends in gene expression of the various treatment groups (Figure 12 – 15). However, results were not statistically significant, and a definitive correlation could not be obtained.

3.5.2. Spearman rank correlation

The Spearman rank correlation coefficient (see equation 1 in section 2.13.) showed a strong correlation (ρ = 0.70) between the live mean cell percentage and the percentage of genes expressed within the sample (Table 5). Additionally, an amended Spearman rank correlation coefficient (see equation 3 in section 2.13.) indicates a very strong correlation (ρ = 0.90) between the total live cell count correlated and the total percentage of genes expressed (Table 6).

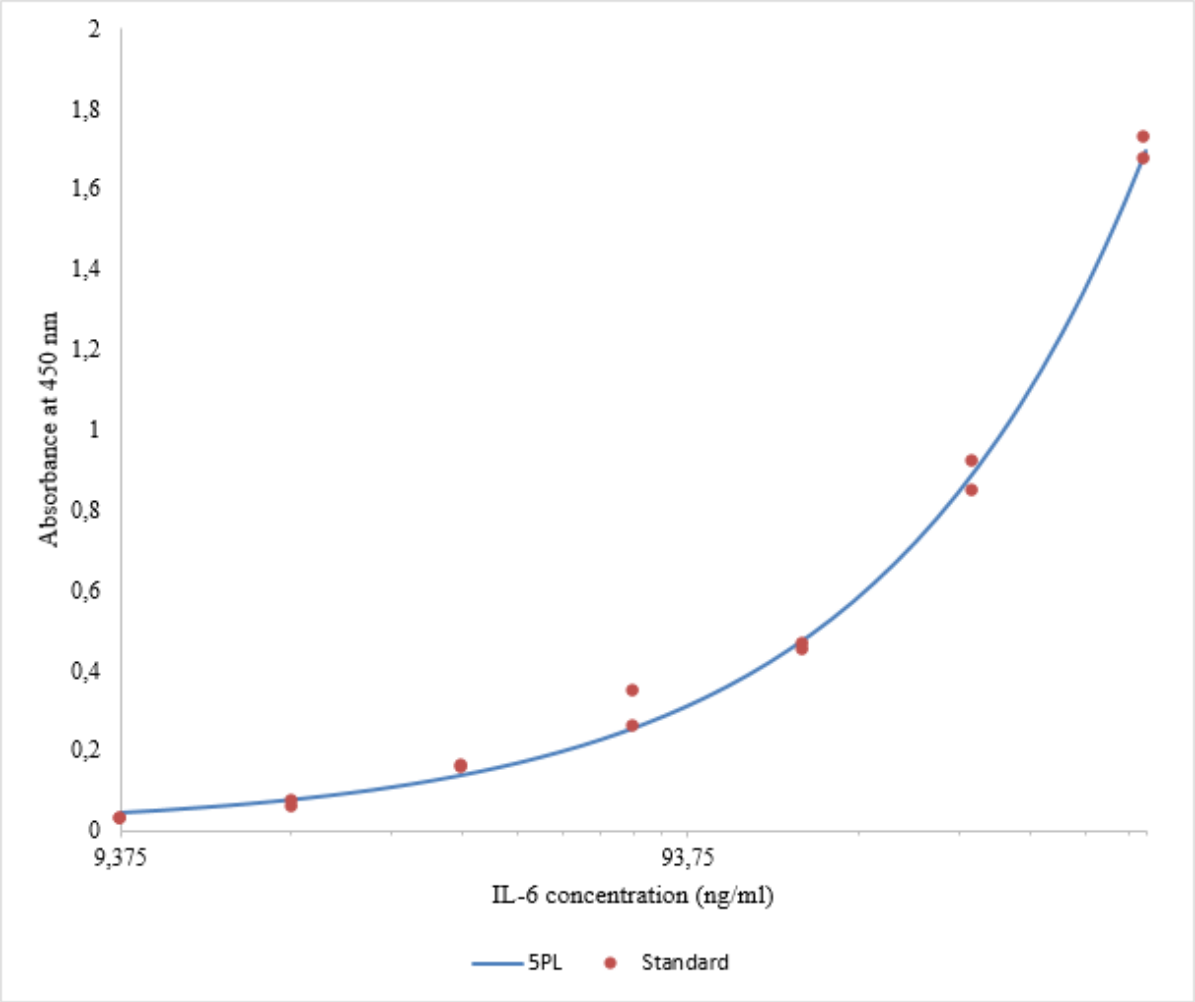


Figure 16: Five-parameter logistic curve expressing to concentration of *IL-6*

The concentration data of the seven standards are shown in duplicate (●) with the line of best fit (—) fitted to a five-parameter logistic curve.

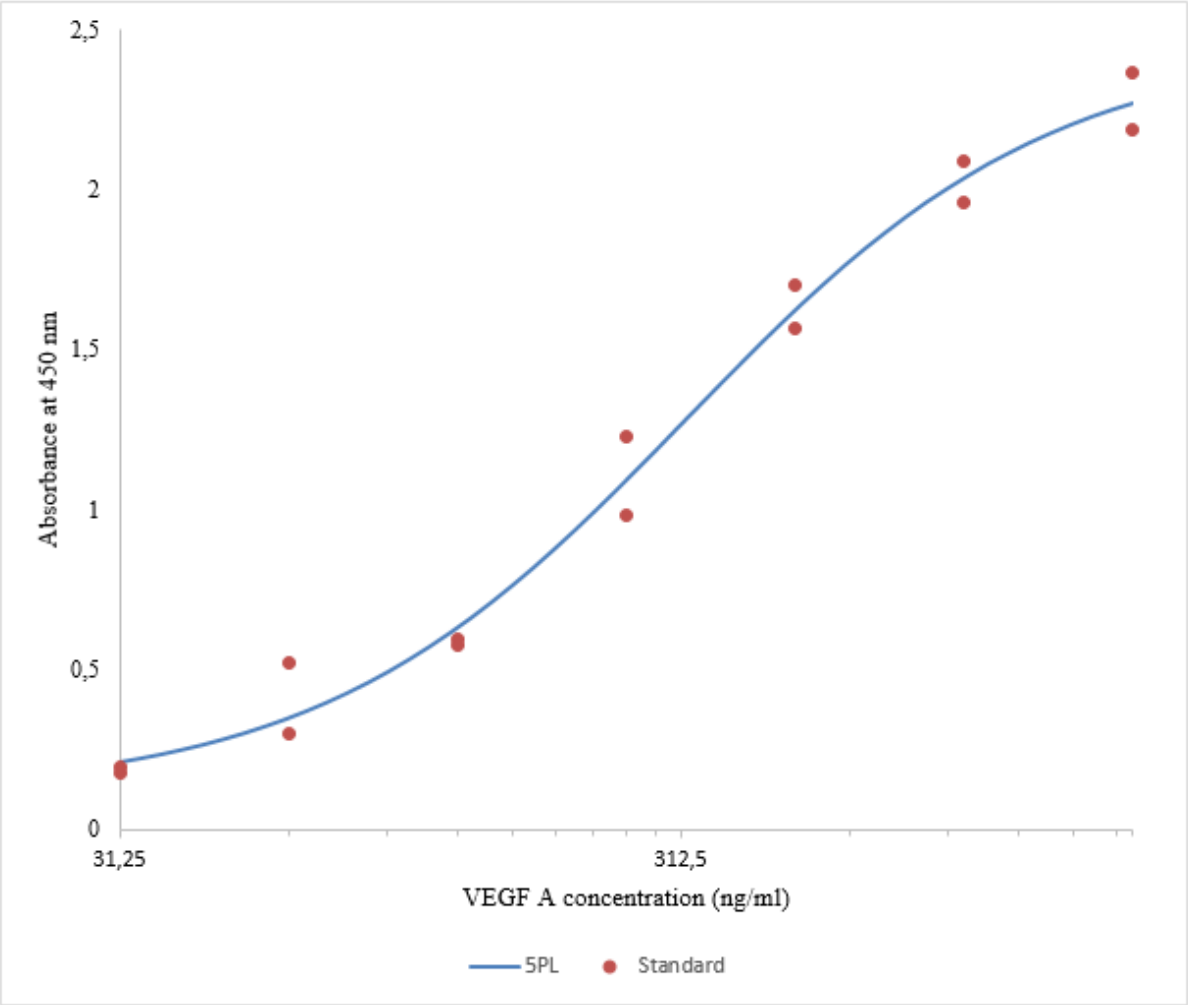


Figure 17: Five-parameter logistic curve expressing to concentration of *VEGF A*

The concentration data of the seven standards are shown in duplicate (●) with the line of best fit (—) fitted to a five-parameter logistic curve.

Table 5: Data for ρ calculation for the correlation of the percentage of live cells with the percentage of genes expressed

n	**Live Cells (%)**	**Rank of Live Cell Percentage (*x*)**	**Genes Expressed (%)**	**Rank of Genes Expressed Percentage (*y*)**	***x* – *y* (*d*)**	***d*²**
Patient 1	16,15	3	66,67	5	-2	4
Patient 2	16,37	4	38,89	3	1	1
Patient 3	13,95	2	33,33	2	0	0
Patient 4	8,34	1	16,67	1	0	0
Patient 5	16,92	5	52,78	4	1	1

n – number of samples; *x* – rank values of the live cell percentage; *y* –rank values of the percentage of genes expressed; *d* – difference between the rank values.

Table 6: Data for ρ calculation for the correlation of the total live cell count with the percentage of genes expressed

n	**Total Live Cell Count**	**Rank of Total Live Cell Count (*x*)**	**Genes Expressed (%)**	**Rank of Genes Expressed Percentage (*y*)**	***x* – *y* (*d*)**	***d*²**
Patient 1	44400	5	66,67	5	0	0
Patient 2	27750	3,5	38,89	3	0.5	0,25
Patient 3	16675	1,5	33,33	2	-0.5	0,25
Patient 4	16675	1,5	16,67	1	0.5	0,25
Patient 5	27750	3,5	52,78	4	-0.5	0,25

n – *number of samples;* x – *rank values of the total live cell count;* y –*rank values of the percentage of genes expressed;* d – *difference between the rank values.*

Chapter 4: Discussion

4.1. Establishment of human endometrial stromal cell lines as a successful *in vitro* model

The ever-evolving and rapidly growing nature of *in vitro* fertilisation research has led to an intense research effort within this field. Progress in this field relies heavily on the availability of viable *in vitro* models as they provide a wealth of evidence within the boundaries of both practical and ethical concerns (Osteen *et al.*, 1989). The methodology for the successful isolation of endometrial cells from endometrial biopsies is well documented (Osteen *et al.*, 1989; Matthews *et al.*, 1992; Zhang *et al.*, 1995; Trundley *et al.*, 2006). The present study aimed to developed a financially feasible methodology for the isolation of HESCs by utilising established protocols (Osteen *et al.*, 1989; Matthews *et al.*, 1992; Zhang *et al.*, 1995; Trundley *et al.*, 2006). Understanding and addressing the complications in establishing *in vitro* HESC models was an essential component of this research; if these complications are not addressed the success of any prospective *in vitro* model will be jeopardised.

Microbial contamination is a serious complication, and can occur in the collection of tissue samples for primary cell line isolation (Vierck *et al.*, 1999). Precautions need to be taken to negate the possibility of contamination; however, this does not guarantee that contamination will not occur (Vierck and Dodson, 1999). The innate protection afforded to tissue is lost once the sample is removed from its natural environment. Strict measures must be taken to prevent the deterioration of the tissue, and to ensure that the loss of this innate protection is not terminal to the sample. In this study, endometrial biopsies were obtained from healthy, reproductively active women undergoing a D&C procedure in the operating theatres at Vitalab. A strict methodology was employed throughout both sample collection and isolation, to limit the introduction of contaminants (see section 2.2). Environmental contaminants were limited through meticulous planning and the preparation of all consumables and work surfaces required during the sample collection and isolation process, as described by Vierck *et al*. (1999). Despite the precautions that were taken, it was observed that endometrial biopsies exhibited high levels of bacterial infection post-isolation. Therefore, additional potential avenues of infection were investigated.

The uterus is situated in the pelvic cavity and is connected, via the cervix, to the vaginal canal. The direct line of contact of the uterus with the vaginal canal results in the possibility of indirect contact of the uterus with the external environment, that may increase the risk of infection

(Sherman, 1999). Under physiological conditions, the uterine tissue is protected from the external environment by the cervix; however, this protection is compromised during the D&C procedure (Davar *et al.*, 2013). Biopsied endometrial samples need to pass through the vaginal canal during extraction. Therefore, these biopsies are exposed to a multitude of dynamic and complex microbial colonies present within the vaginal canal (Larsen and Monif, 2001), and results in an increase in the probability of samples being infected during collection and isolation. The effect of endogenous infection within samples was limited by increasing the concentration of antimicrobials within the tissue collection media (see section 2.2. and 3.1.1.). Observations indicated that this method successfully decreased the levels of infection (see section 3.1.1.), thus enabling the isolation of stromal cells to proceed normally.

Observations from this study also indicate that blood has deleterious effects on HESC isolation (see section 3.1.2.). The deleterious effects result from blood-related infection as well as coagulation. Blood is a potential host to a multitude of microorganisms; therefore, blood can carry an endogenous risk of infection (Weinstein and Weinstein, 2003). Bikfalvi (2004) has shown that platelet factor 4 (PF4), a chemokine released from platelets during coagulation, inhibits the function of collagenase in tissue culture. Inhibition of collagenase is detrimental because it is essential to ensure a larger yield of cells post-isolation (Bikfalvi, 2004). The findings presented here corroborate the findings by both Vierck *et al.* (1999) and Bikfalvi (2004), since the washing of samples in PBS reduced both the infection rates post-isolation and visible coagulation during enzymatic tissue digestion (see section 3.1.2.).

Optimisation of the tissue collection and HESC isolation procedures limited the effects of infection and coagulation, and resulted in the successful establishment of an *in vitro* HESC model. The success of the *in vitro* HESC model was shown through the use of light microscopy to observe the characteristic morphological alterations that these cells are expected to undergo *in vitro*. Isolated cells from endometrial biopsies show rapid attachment to tissue culture plasticware, as the cells had attached after 24 – 48 hours (Figure 2). These findings correlate with those of Fernández-Shaw *et al.* (1992), who showed that cells exhibit substantial adherence to culture dishes, following 24 – 48 hours of culture. Adherent HESCs express a long and spindle-like morphology with cytoplasmic projections extending throughout the culture flask (Figures 2 and 3), which is in agreement with the known cellular phenotypes during this period (Fernández-Shaw *et al.*, 1992; Zhang *et al.*, 1995; Arnold *et al.*, 2001; Dunn *et al.*, 2003; Krikun *et al.*, 2004; Kajihara *et al.*, 2013). Human endometrial epithelial cells appeared smaller, and established small whorl-like clusters of cells (Figure 2). This finding is in agreement with existing literature (Fernández-Shaw *et al.*, 1992; Zhang *et al.*, 1995). The

results obtained here indicate that HESCs exhibit a greater propensity for early attachment than human endometrial epithelial cells (Figures 2 and 3). HESCs attach with greater affinity to plastic ware, and proliferate better than human endometrial epithelial cells (Arnold *et al*., 2001). The use of untreated tissue culture plastic ware could, therefore, have resulted in the greater propensity for early attachment displayed by HESCs. Additionally, early attachment assisted in purifying HESCs, because growth media was discarded after the initial 48 hours of culture, thus removing the unattached endometrial epithelial cells. The evidence presented here indicates that confluency alters the appearance of HESCs to a more polygonal morphology (Figures 3 and 4), a characteristic that has also been observed in other studies (Dorman *et al.*, 1982; Fernández-Shaw *et al.*, 1992; Arnold *et al.*, 2001). Figure 2 clearly indicates that HESCs express different morphology, dependent on their location within the colony. Cells on the periphery exhibit typical stromal cell morphology, and become more tightly packed towards the centre of the colony. However, the rate at which HESCs reach confluency can vary. The HESCs established in this study consistently reached confluency between 8 – 10 days in culture, and research suggests that HESCs can reach confluency anywhere between 7 – 14 days (Dorman *et al.*, 1982; Fernández-Shaw *et al.*, 1992). Differences in the rate at which these cells reach confluency *in vitro* can be explained by the fact that initial cell numbers, and overall cell viability, may vary between samples (Fernández-Shaw *et al.*, 1992). At 80% confluency, HESCs exhibit an almost entirely polygonal morphology (Figure 4), which closely resembles HESCs found during the secretory phase of the menstrual cycle *in vivo* (Dorman *et al*., 1982). It has been proposed that these polygonal HESCs can be described as predecidual, because the cells exhibit a similar structure and ultrastructure to decidualised HESCs even in the absence of the steroid hormones (Dorman *et al*., 1982).

The results from the light microscopy study (Figures 2 - 4) indicate that a successful *in vitro* model for HESCs was established. Additionally, the samples obtained were able to undergo successful consecutive passaging. However, even though a successful model was established, the isolated HESC samples displayed poor viability following cryopreservation.

4.2. Factors affecting cell viability

Cell viability is an essential requirement for any research using cells as the sample medium (Sheridan *et al.*, 1998). If cell viability is decreased, the downstream applications are limited. As discussed in section 4.1., the isolation of HESCs was successful; however, the cells expressed poor viability following cryopreservation (Table 1 and Figures 5 - 10). In an attempt

to revive cells and improve cell viability, extensive troubleshooting was conducted on stock samples of passaged HESC. However, troubleshooting proved unsuccessful, and had to be discontinued. Stock samples needed to be maintained to ensure that the research could progress, as the collection and isolation of new tissue samples was not a viable option for this study.

The cryopreservation technique used could provide a possible explanation for the low viability rates of cells. Cryopreservation is an essential technique in cell culture. The ability to store cells for extended periods of time allows for the downstream use of cells for a variety of techniques (Szóstek *et al.*, 2012; Isachenko *et al.*, 2013; Chen *et al.*, 2016). It is well documented that the formation of ice crystals in cells is an inherent effect of cryopreservation (Deller *et al.*, 2014). Ice crystal formation can have detrimental effects on cell populations because of mechanical damage and osmotic shock. Additionally, cell lysis can occur during the thawing process (Deller *et al.*, 2014). In an attempt to reduce ice crystal formation, cryopreservation solutions are used containing organic solvents such as DMSO, since these are recognised to promote a state known as vitrification. Vitrification refers to a state in which cells are frozen in a glassy state, and ice-crystal formation is prevented (Szóstek *et al.*, 2012; Deller *et al.*, 2014; Chen *et al.*, 2016). Cells used in this study were cryopreserved in media containing DMSO and stored at -80°C (see Section 2.4.). However, it has been shown that cells have improved viability when frozen and stored using liquid nitrogen at -196°C, the consequence of which is a rapid attainment of the glassy state (Ryan, 2004). Freezing samples in liquid nitrogen ensures the total halting of all biological processes within cells, whereas storage at -80°C only slows the progression of these processes (Ryan, 2004). Therefore, cells will eventually lose viability when frozen and subsequently stored for extended periods of time at -80°C. The samples used in this study were stored at -80°C, and all presented similar viability rates, even though their storage time at -80°C differed from two months to longer than twelve months. This is important, as the samples stored at -80°C for longer than twelve months should have exhibited a significantly lower cell viability than those stored for a period of two months (Qiagen, 2010). Therefore, the low viability and attachment rates of HESCs in this study may have been in part due to not storing the samples using liquid nitrogen. However, the similar viability rates of samples regardless of storage time suggests a more complex reason behind the poor attachment and viability rates observed within the samples.

HESCs are fibroblasts found within the uterus, the function of which is the secretion of a variety of cytokines and chemokines essential in cellular communication (Tabanelli *et al.*, 1992; Brar *et al.*, 2001). The intramolecular communication of HESCs, and the intermolecular communication of HESCs with neighbouring cells within the uterus is highly regulated and

precise (Kajihara *et al.,* 2013). Recently it has been shown that cryopreservation negatively affects, and even inhibits, the secretory function of cells (Cai *et al.*, 2017), including HESCs (Bochev *et al.,* 2016). The HESCs used in this study show an inhibition of their secretory function with regards to *VEGF A* and *IL-6* (see Section 3.4.). In both ELISAs, the supernatant of each sample indicates that the concentrations of both *VEGF A* and *IL-6* were immeasurable. This evidence correlates with the research of Bochev *et al.*, (2016), because the authors discuss that cryopreservation significantly reduces the concentration of *IL-6* secreted by HESCs, when compared to fresh HESC samples. Additionally, inhibition of the inherent secretory ability of cells has downstream deleterious effects on the overall function, growth and proliferation (Bochev *et al.*, 2016; Cai *et al.*, 2017). Therefore, the negative effects conferred by cryopreservation could have resulted in the low cell viability and attachment rates observed in the HESCs established in this study. It is important to note that future studies involving HESCs should consider the effects of cryopreservation, in order to establish a more effective cryopreservation protocol.

The effects of cell viability on gene expression levels were assessed to gain an understanding of the implications of poor cell viability. The results show a strong correlation between the percentage of viable cells and the total overall expression of genes (see Section 3.5.2.), and that a low live cell percentage results in poor gene expression (see Section 3.5.2.). It is unknown whether live cell percentage affects gene expression, or whether the lower number of cells present in samples affects gene expression. It is well established that a low initial cell number results in a lower mRNA yield (Qiagen, 2010; Viet-Phuong Le *et al*., 2015), and that low mRNA concentrations directly affect Real-Time qRT-PCR gene expression profiles (El-Khoury *et al.*, 2016). Therefore, perhaps gene expression is low in samples with low cell counts because these samples have inherently lower concentrations of mRNA, resulting in a reduced gene expression profile (Qiagen. 2010; Viet-Phuong Le *et al*., 2015; El-Khoury *et al*., 2016).

4.3. The importance of primer design in Real-Time Quantitative Reverse Transcription PCR (Real-Time qRT-PCR)

The poor cell viability of the samples used in this study severely affected downstream applications such as Real-Time qRT-PCR. Therefore, statistically significant data describing the effect of hormonal stimulation, from E_2 and MPA, on gene expression could not be obtained. However, this study still successfully identified the potential role that these hormones

have on gene expression within HESCs through successful primer design and Real-Time qRT-PCR.

The designing of viable primers is an integral step to ensure both the success and validity of Real-Time qRT-PCR. There is much debate surrounding the issue of whether or not primers should be designed on a per assay basis or purchased directly from commercial suppliers (Bustin and Huggett, 2017). In a recent review conducted by Bustin & Huggett (2017), it was suggested that primers should almost always be designed on a per assay basis because commercially acquired primers are not experimentally validated for specific assay conditions. Furthermore, the performance of a specific assay is highly dependent on the overall experimental design used. The guidelines described in the Minimum Information for Publication of Quantitative Real-Time PCR Experiments (MIQE) were used for successful primer design (Bustin *et al*., 2009). The primers designed in this study were not scientifically validated to the extent described by Bustin & Huggett (2017). However, the primers were sufficiently validated because they showed negligible differences in Cq values, and the duplicate samples displayed only single peak melting temperatures (Figure 11). Primers must be appropriately validated for specific experimental conditions to ensure that the Real-Time qRT-PCR results are significant (Robertson and Walsh-Weller, 1998). Real-Time qRT-PCR has been established as a critical research and analysis tool in a multitude of scientific fields (Robertson and Walsh-Weller, 1998; Valasek, 2005; Deepak *et al.*, 2007; Kralik and Ricchi, 2017). Experimental data acquired from Real-Time qRT-PCR gives quantitative evidence which is both sensitive and specific, two essential criteria required for understanding the dynamics of gene expression within the human body (Deepak *et al.*, 2007). Real-Time qRT-PCR can produce data which is statistically significant, however, sufficient amounts of high quality mRNA is required for accurate results (Bustin *et al.*, 2009).

Unfortunately, the results could not be statistically validated because the isolated mRNA was neither sensitive nor specific. Despite these complications, the potential role of hormones on gene expression within HESCs was still successfully identified.

4.4. E_2 and MPA on receptor expression

ERα plays an important role within the endometrium (Kastner *et al.*, 1990). This study could not show the effect of E_2 on the receptor; however, this effect is well documented (Kastner *et al.*, 1990; Couse *et al.*, 1997; Kuiper *et al.*, 1997; Classen-Linke *et al.*, 1998). E_2 acts by increasing the expression of *ESR-α* and evidence suggests that this upregulation is essential for

the menstrual cycle to proceed (Kastner *et al*., 1990; Couse *et al*., 1997; Kuiper *et al*., 1997; Classen-Linke *et al*., 1998) through processes such as angiogenesis (Simoncini *et al.*, 2006). Simoncini *et al.* (2006) showed that E_2's role in activating ESR-α establishes a favourable environment allowing for the faster migration of endothelial cells to non-vascular areas, thus ensuring angiogenesis can occur. Furthermore, the upregulation of *PGR* is linked to the increasing levels of *ESR-α* (Kastner *et al*., 1990). In the present study, MPA appeared to have little effect on *ESR-α* expression. The data presented here (see section 3.3.5.2.) contradicts the evidence presented by Giulianelli *et al*. (2012), who found that MPA induced both the expression and activation of *ESR-α* in human T47D and c4-HD cell lines. The differences could have resulted from the altered gene expression and functionality of the progestin-dependent cancer cell lines used in this study (Giulianelli *et al.*, 2012).

The *PGR* is an essential mediator within HESCs during the menstrual cycle (Gao, 2000). Evidence presented in Figure 13 shows that the *PGR* is minimally increased in the presence of E_2. However, it is accepted that *PGR* is upregulated in the presence of E_2 as a method of preparing the uterus for the secretory phase of the menstrual cycle (Kastner *et al*., 1990; Ohno and Fujimoto, 1998).

4.5. E_2 and MPA on growth factor expression

TGF-β_1 is an essential protein within the endometrium due to its function during the tissue remodelling process (Jones *et al*., 2006b). This protein is known to regulate apoptosis within stromal cells which is particularly important during decidualisation and embryo implantation (Chatzaki *et al.*, 2003). This study showed that *TGF-*β_1 is upregulated in the presence of E_2 within HESCs. The findings are similar to those reported by Takahashi *et al*. (1994) where *TGF-*β_1 expressed upregulation within the stroma of murine models in the presence of oestrogen. Similar findings have been reported in human models as well. Stevenson *et al*. (2008) reported that human dermal fibroblasts expressed an upregulation and increased secretion of *TGF-*β_1 in the presence of E_2. The upregulation of *TGF-*β_1 in stromal cells is linked to the regulation of apoptosis and proliferation. It has been experimentally demonstrated that stromal cells undergo both proliferation and apoptosis during the menstrual cycle (Arends, 1999; Chatzaki *et al.*, 2003). Both proliferation and apoptosis must be highly regulated to ensure that they are maintained at acceptable levels. These processes are essential in controlling important physiological phenomena such as menstrual cycle progression and blastocyst implantation (Arends, 1999; Chatzaki *et al.*, 2003).

The functional importance of *VEGF A* is well documented (Rizk *et al*., 1997; Huang, Liu & Dawood, 1998; Sharkey *et al*., 2000; Jensen *et al*., 2010; Srivastava *et al*., 2013) and there is strong evidence that both E_2 and MPA regulate its expression within HESCs (Zhang, Rees and Bicknell, 1995; Huang, Liu and Dawood, 1998). The evidence depicted in Figure 15 implies that *VEGF A* expression is increased in the presence of either E_2 or MPA. These data correlate with the results published by Zhang, Rees & Bicknell (1995) who showed a 2.5-fold increase in the expression of *VEGF A* of HESCs in the presence of E_2 and a 2-fold increase in the presence of MPA. Lower expression levels in this research may in part be due to the lower incubation times of E_2 and MPA in culture (2 days) in comparison to those used by Zhang, Rees & Bicknell (1995) (9 days). Higher levels of *VEGF* during hormonal stimulation has been linked to the regeneration of the endometrium after menstruation (Huang, Liu and Dawood, 1998). The increase in expression of *VEGF A* in the presence of either oestrogen or progesterone is linked to the functional importance that this molecule has in angiogenesis. Research has shown that there is a strong correlation to the effect oestrogen has on *VEGF A* expression and how this expression is critical for oestrogen induced vascular remodelling of the endometrium (Fraser *et al*., 2008). Girling *et al.* (2007) emphasised the importance of the relationship between progesterone and *VEGF A* through murine models. It was found that in the presence of a *VEGF* antiserum there was a significant reduction in progesterone-induced endothelial cell proliferation.

This study was unable to establish the effect E_2 and MPA have on IL-6 within HESCs. However, research conducted by Von Wolff *et al.*, (2002) show that this cytokine is differentially expressed within the uterus during the menstrual cycle, with its maximal expression occurring during the late secretory phase. The study alludes to this differential expression being imperative to IL-6s role as a multi-functional cytokine.

4.6. Conclusion

Understanding the effect of both E_2 and MPA on HESCs *in vitro* is essential in gaining perspective on the individual roles of these hormones during the menstrual cycle. The data presented in this study indicates that E_2 and MPA are important for dynamic receptor and growth factor expression of HESCs. However, the cryopreservation technique that was used prevented conclusive validation of the specific mechanism employed by E_2 and MPA in the regulation of receptor and growth factor expression of HESCs *in vitro*. The usefulness of data obtained in this study is two-fold. Firstly, a successful protocol has been established for the use

of HESC lines as a successful *in vitro* model. Secondly, the importance of cryopreservation for maintaining viable cells that can be used in downstream applications has been highlighted. Therefore, this study adds to the technical knowledge-base of cell culture techniques, and provides insight into the individual roles of menstrual cycle hormones. This insight improves our understanding of the affect these hormones have when acting in conjunction, on phenomena such as HESC decidualisation.

APPENDIX

List of figures

Appendix Figure 1: Human Ethics Certificate 61
Appendix Figure 2: Blank consent form 62

List of tables

Appendix Table 1: Transcript variants of *TGF-β*1 67
Appendix Table 2: Designed forward and reverse primers for *TGF-β*1 68
Appendix Table 3: Transcript variants of *TGF-β*2 69
Appendix Table 4: Designed forward and reverse primers for *TGF-β*2 71
Appendix Table 5: Transcript variants of *TGF-β*3 72
Appendix Table 6: Designed forward and reverse primers for *TGF-β*3 73
Appendix Table 7: Transcript variants of *ESR-α* 75
Appendix Table 8: Designed forward and reverse primers for *ESR-α* 76
Appendix Table 9: Transcript variants of *ESR-β* 77
Appendix Table 10: Designed forward and reverse primers for *ESR-β* 79
Appendix Table 11: Transcript variants of *PGR* 80
Appendix Table 12: Designed forward and reverse primers for *PGR* 82

Appendix A: Ethical clearance certificate (M1511106)

R14/49 Mr Kyle Daniel Wiid

HUMAN RESEARCH ETHICS COMMITTEE (MEDICAL)

CLEARANCE CERTIFICATE NO. M1511106

NAME: (Principal Investigator)	Mr Kyle Daniel Wiid
DEPARTMENT:	Anatomical Sciences University of the Witwatersrand
PROJECT TITLE:	Profiling of Transforming Growth Factor Beta (&) Isoforms in Isolated Human Endometrial Stromal Cells During Hyperstimulation
DATE CONSIDERED:	Adhoc
DECISION:	Approved unconditionally
CONDITIONS:	
SUPERVISOR:	Aleksandra Jovanovic
APPROVED BY:	Professor A Dhai, Co-Chairperson, HREC (Medical)
DATE OF APPROVAL:	21/12/2015

This clearance certificate is valid for 5 years from date of approval. Extension may be applied for.

DECLARATION OF INVESTIGATORS

To be completed in duplicate and **ONE COPY** returned to the Secretary in Room 10004, 10th floor, Senate House, University.
I/we fully understand the conditions under which I am/we are authorized to carry out the above-mentioned research and I/we undertake to ensure compliance with these conditions. Should any departure be contemplated, from the research protocol as approved, I/we undertake to resubmit the application to the Committee. **I agree to submit a yearly progress report**.

Principal Investigator Signature Date

PLEASE QUOTE THE PROTOCOL NUMBER IN ALL ENQUIRIES

Appendix Figure 1: Human Ethics Certificate

Appendix B: Blank consent form and information sheet

CONSENT FORM

SCHOOL OF ANATOMICAL SCIENCES, UNIVERSITY OF THE WITWATERSRAND, JOHANNESBURG

Donation of the part of uterine tissue taken from your uterine lining during the dilation and curettage procedure

Tissue sample to be used for the purpose of research

I, (Full name in block letters)

Consent to the donation of the tissue sample that will be taken from my uterine lining during the dilation and curettage (D&C) procedure which I am to undergo.

I understand that this tissue sample will be used for the purpose of isolating uNK cells and/or endometrial stromal cells as described in the project information sheet which I have read.

I understand that I will receive no remuneration in lieu of this donation. I understand too, that this is entirely voluntary.

Signed: _____

At _____ on the _____

(Name of the hospital)

Witnesses:

Name	Name
Signature	Signature
Date	Date

Appendix Figure 2: Blank consent form

INFORMATION FORM (UTERINE TISSUE DONATION)

THE ROLE OF LYMPHOCYTES IN UTERINE RECEPTIVITY FOR IMPLANTATION

Investigator: Mrs. Aleksandra Jovanović

Co-Investigator: Mr. Kyle Wiid

Dear patient,

Our names are Aleksandra Jovanović and Kyle Wiid. We are research scientists at the School of Anatomical Sciences, the University of the Witwatersrand, Johannesburg. We are conducting research which investigates the effects of the exogenous gonadotropins (hormones that are routinely used in assisted reproductive technologies for patients who have problems conceiving) on the expression of certain lymphocytes (white blood cells) called uterine Natural Killer (uNK) cells as well as on endometrial stromal cells in the uterus, during the time when the embryo normally implants.

uNK cells constitute the predominant lymphocyte subtypes present in the uterine endometrium at the time of implantation and in early pregnancy. uNK cells have the role in secretion of growth factors and other important molecules as their capacity to promote and direct embryo invasion and endometrial vascular growth. uNK cells are involved in spiral artery remodelling which allows adequate maternal adaptations and successful pregnancy outcome.

Endometrial stromal cells are fibroblast like cells found within the uterus. During the menstrual cycle these cells undergo a process known as decidualisation which alters these cells both structurally and functionally. These differentiated endometrial stromal cells, or decidual stromal cells, become rounded, acquire myofibroblast characteristics and secrete a variety of cytokines. These changes are essential for both embryo implantation and placentation.

Differences in the normal expression of uNK cells and the inhibition of decidualisation of endometrial stromal cells in the uterus following hyperstimulation (the exogenous administration of gonadotropins), may indicate the requirement of these cells in the successful embryonic implantation of the embryo. The findings from this project will broaden the understanding of the function and dynamics of these cells and their interaction with the uterine lining.

We are inviting you to participate to our study

We are asking permission to use a piece of the tissue from the uterine lining which is the tissue doctors are already taking from your uterus during the dilation and curettage (D&C) procedure. There are no extra procedures involved. We will use this tissue to do laboratory experiments,

which would inform how exogenous hormones work in the human uterus during initial stages of implantation and whether they affect the expression of uNK cells.

Please Note

1) The tissue we use would only be used for this study.

2) If you agree to participate in this study you will not benefit directly in any way. Also there will be no direct result of the analysis of your sample as we will group many results from samples together before we will be able to see a pattern. We hope that our study may contribute to new and better ways of combating infertility in women.

3) As with any other medical records your details will not be used by or disclosed to anyone. We will allocate you a number and never use your name or any other information which would allow you to be identified. All records are anonymous.

4) The researchers in this study have no financial interests or will not gain financially by your participation in this study.

5) If you do not want to participate in this study you will continue to receive the best available treatment. Further if you agree and later change your mind we will destroy all of the samples you have given us and remove your record from our information sheet.

6) The study has been approved by the Human Ethics Committee of the University of the Witwatersrand who can be contacted on 011-7171234.

If you are willing to volunteer to take part in this study we would ask you to sign this document stating that you are volunteering and that we have explained our study to you.

Patient signature: Date

_____

Study Number _____

Investigator signature: Date

_____

Appendix C: PBS Stock Solution

a. Ingredients:

i.	NaCl	16 g
ii.	$Na_2 4PO_4.H_2O$	2.3 g
iii.	KCl	0.4 g
iv.	KH_2PO_4	0.4 g
v.	Distilled Water	2 l

b. Method:

i. Combine all ingredients together in a 2 L conical flask and ensure it is mixed thoroughly.
ii. Establish a pH of 7.4.
iii. Autoclave PBS pH 7.4.
iv. Store at 4 °C until required.

Appendix D: Primer Design

Primers were designed for *TGF-β*$_1$, *TGF-β*$_2$, *TGF-β*$_3$, *ESR-α*, *ESR-β*, *PGR* and *VEGF A*. All transcript variants were considered during primer design to ensure that the gene of interest was accurately and precisely targeted.

***TGF-β*1:**

*TGF-β*1 (NM_000660.6) has no registered transcript variants (Table 2). Therefore, the full mRNA nucleotide sequence was used in order to establish primers. The *TGF-β*1 nucleotide sequence is 2 741 base pairs long (Table 2).

BLAST search was performed on the sequence and similarities were found within *TGF-β*1 and other homologous sequences. Subsequently, PrimerQuest© (Integrated DNA Technologies) was used to evaluate the nucleotide sequences. Once designed, the primers were analysed by performing a BLAST search which showed that both entities were unique to *TGF-β*$_1$ (Table 3).

***TGF-β*$_2$:**

*TGF-β*2 has two known transcript variants: transcript variant 1 (NM_001135599.3) and transcript variant 2 (NM_003238.4) (Table 4). Transcript variant 1 has a nucleotide sequence 6 016 base pairs long whereas transcript variant 2 has a nucleotide sequence 5 932 base pairs long. A sequence alignment was run between the two sequences to establish if an mRNA sequence was present in both transcript variants. Transcript variant 1 was used as the query sequence due to its longer length (6 016) compared to transcript variant 2 (5 932) (Table 4).

Appendix Table 1: Transcript variants of *TGF-β*1

Transcript Variant	Similarity (%)	Number of base pairs	Query cover of alignment (%)	Base pair alignment range
1	100	2 741	100	1 – 2 741

Appendix Table 2: Designed forward and reverse primers for *TGF-β*1

Type	Sequence	Start	Length (bp)	Tm (ºC)	GC (%)	Amplicon (bp)
Forward Primer	CCTGCCTGTCTGCACTATTC	2 243	20	62.29	55	
Reverse Primer	TGCCCAAGGTGCTCAATAAA	2 340	20	62.41	45	
Product						98

Appendix Table 3: Transcript variants of *TGF-β2*

Transcript Variant	**Similarity (%)**	**Number of base pairs**	**Query cover of alignment (%)**	**Base pair alignment range**
1	100	3 510	100	1 – 6 016
2	100	3 466	98	1 – 1 764; 1 908 – 6 016

Transcript variant 2 had a query cover of 98% when compared to transcript variant 1. This coverage was divided over two regions and it was found that the base pairs between 1 764 and 1 908 of transcript variant 1 were dissimilar. Due to the split coverage of the alignment, the nucleotide sequence with the greater amount of base pairs (1 908 – 6 016) was chosen. A BLAST search was performed on the chosen nucleotide sequence and the results showed a similarity to *TGF-β_2* and other related sequences (Table 4).

Once the unique similarity was established, the nucleotide sequence was analysed by PrimerQuest© (Integrated DNA Technologies). Subsequently, a BLAST search confirmed that the designed primers, when analysed as separate entities, were unique only to *TGF-β_2* (Table 5).

***TGF-β_3*:**

TGF-β_3 has three known transcript variants (NM_003239.4, NM_001329939.1 and NM_001329938.1) (Table 6). A sequence alignment was performed to compare both transcript variant 2 (NM_001329939.1) and 3 (NM_001329938.1) to transcript variant 1 (NM_003239.4), in order to obtain an mRNA sequence which was present in all three transcript variants. Transcript variant 1 was chosen as the query sequence as it contained a higher number of base pairs (3510) that are more similar to all transcripts than transcript variant 2 (3 466) and transcript variant 3 (2 362) (Table 6).

Transcript variant 2 had a 92% query cover when compared to transcript variant 1. The alignment of base pairs occurred between base pairs 262 – 3 510 of transcript variant 1. Transcript variant 3 had a 58% query cover when compared to transcript variant 1. The alignment occurred between base pairs 1 – 2055 of transcript variant 1. Consequently, the sequence which had a query cover of 100% for all three transcript variants was 1 793 base pairs long and between 262 – 2 055 of transcript variant 1. Subsequenly, a BLAST search was performed on the chosen nucleotide sequence and the results showed that the chosen sequence only showed similarity to *TGF-β_3* and related sequences (Table 6).

Once the unique similarity was established, the nucleotide sequence was analysed by PrimerQuest© (Integrated DNA Technologies). Subsequently, a BLAST search confirmed that the designed primers, when analysed as separate entities, were unique only to *TGF-β_3* transcript variants (Table 7).

Appendix Table 4: Designed forward and reverse primers for *TGF-β2*

Type	Sequence	Start	Length (bp)	Tm (ºC)	GC (%)	Amplicon (ºC)
Forward Primer	CGGAGGTGATTTCCATCTACAA	1 612	22	61.96	45.46	
Reverse Primer	AAGGGCGGCATGTCTATTT	1 750	19	61.93	47.37	
Product						139

Appendix Table 5: Transcript variants of *TGF-β3*

Transcript Variant	**Similarity (%)**	**Number of base pairs**	**Query cover of alignment (%)**	**Base pair alignment range**
1	100	3 510	100	1 – 3 510
2	100	3 466	92	262 – 3 510
3	100	2 362	58	1 – 2 055

Appendix Table 6: Designed forward and reverse primers for *TGF-β*3

Type	Sequence	Start	Length (bp)	Tm (ºC)	GC (%)	Amplicon (bp)
Forward Primer	GAGAGTCAAGTCCAAGGGAATG	119	22	62.23	50	
Reverse Primer	CTGCTCCGGAAAGCTGTTAT	204	20	62.19	50	
Product						86

***ESR-α*:**

ESR-α has seven known transcript variants: Transcript variant 1 (NM_000125.3), 2 (NM_001122740.1), 3 (NM_001122741.1), 4 (NM_001122742.1), 5 (NM_001291230.1), 6 (NM_001291241.1) and 7 (NM_001328100.1) (Table 8). All seven variants have nucleotide sequences of varying length with transcript variant 4 having the longest (6 466) and transcript variant 7 the shortest (5 421). Due to its length, transcript variant 4 was chosen as the query sequence used in the alignment of *ESR-α*'s transcript variants (Table 8).

Transcript variants 1, 2, 3 and 7 showed a 100% similarity when compared to transcript variant 4 whereas transcript variants 5 and 6 were 99% similar to transcript variant 4. All transcript variants had a 95% query cover against transcript variant 4 except for transcript variant 7 which showed a 14% query cover. The area of alignment of transcript variant 7 was 920 base pairs long and was found in the region between 821 – 1 740 of transcript variant 4. Transcript variant 7 had a 100% alignment on all six other *ESR-α* transcript variants and as a result was used in its entirety for the primer design. A BLAST search was performed on the nucleotide sequence of transcript variant 7 and it was found that major similarities were only present in *ESR-α* and other related sequences (Table 8).

Once the unique similarity was established, the nucleotide sequence was analysed by PrimerQuest© (Integrated DNA Technologies). Subsequently, a BLAST search confirmed that the designed primers, when analysed as separate entities, were unique only to *ESR-α* transcript variants (Table 9).

***ESR-β*:**

ESR-β has seven known transcript variants: Transcript variant a (NM_001437.2), b (NM_001040275.1), d (NM_001214902.1), f (NM_001271876.1), g (NM_001271877.1), k (NM_001291712.1) and l (NM_001291723.1) (Table 10). All seven of *ESR-β* transcript variants have nucleotide sequences of differing lengths. Transcript variant k had the longest nucleotide sequence (4 037) and transcript variant g the shortest (1 518). Transcript variant k was selected as the query sequence for transcript variant alignment as a result of its length (Table 10).

Appendix Table 7: Transcript variants of *ESR-α*

Transcript Variant	**Similarity (%)**	**Number of base pairs**	**Query cover of alignment (%)**	**Base pair alignment range**
1	100	6 330	95	299 – 6 466
2	100	6 357	95	301 – 6 466
3	100	6 314	95	300 – 6 466
4	100	6 466	100	1 – 6 466
5	99	6 320	95	300 – 6 466
6	99	6 311	95	300 – 6 466
7	100	5 421	14	821 – 1 740

Appendix Table 8: Designed forward and reverse primers for *ESR-α*

Type	Sequence	Start	Length (bp)	Tm (°C)	GC (%)	Amplicon (bp)
Forward Primer	GCTTCGATGATGGGCTTACT	568	20	61.99	50	
Reverse Primer	CCTGATCATGGAGGGTCAAATC	678	22	62.43	50	
Product						109

Appendix Table 9: Transcript variants of *ESR-β*

Transcript Variant	**Similarity (%)**	**Number of base pairs**	**Query cover of alignment (%)**	**Base pair alignment range**
a	100	2 169	37	1 637 – 3 134
b	100	2 470	51	1 637 – 3 716
d	100	2 407	51	1 639 – 3 716
f	100	1 724	37	1 639 – 3 155
g	100	1 518	30	1 639 – 2 681 2 948 – 3 134
k	100	4 037	100	1 – 4 037
l	99	2 745	67	1 – 657 1 633 – 3 716

Transcript variants a, b, d, f and g were 100% similar to transcript variant k whereas transcript variants l expressed 99% similar to transcript variant k. Transcript variant l had the highest query cover (67%) when compared to transcript variant k, which was divided over two regions; region 1 was between 1 – 657 and region 2 between 1 633 – 3 716. Transcript variants b and d both presented 51% alignment to transcript variant k. Transcript variant b's alignment occurred in region 1 637 – 3 716 and transcript variant d's alignment occurred in region 1 639 – 3 716. Transcript variants a and f both aligned to transcript variant k by 37%. Transcript variant a's alignment occurred in the region between 1 637 – 3 134 and transcript variant f's alignment occurred in the region between 1 639 – 3 155. Transcript variant g showed the lowest query cover when compared to transcript variant k (30%). This coverage was divided into two regions; region 1 was between 1 639 – 2 681 and region 2 between 2 948 – 3 134. The nucleotide sequence which was similar in all seven transcript variants was found between 1 639 – 2 681 of transcript variant k and was 1 043 base pairs long. A BLAST search was performed on the nucleotide sequence, and major similarities were only present in *ESR-β* and other related sequences (Table 10).

Once the selective similarity to *ESR-β* transcript variants were established, the nucleotide sequence was analysed by PrimerQuest© (Integrated DNA Technologies). Subsequently, a BLAST search confirmed that the designed primers, when analysed as separate entities, were unique only to *ESR-β* transcript variants (Table 11).

***PGR*:**

PGR has four known transcript variants; 1 (NM_001202474.3), 2 (NM_000926.4), 3 (NM_001271161.2) and 7 (NM_001271162.1). Transcript variant 2 has the longest sequence (13 037) and transcript variant 7 the shortest (10 957). Transcript variant 2 was used as the query sequence for transcript variant alignment of *PGR* due to its greater length compared to the other transcript variants (Table 12).

Appendix Table 10: Designed forward and reverse primers for *ESR-β*

Type	Sequence	Start	Length (bp)	Tm (°C)	GC (%)	Amplicon (bp)
Forward Primer	GATCGCTAGAACACACCTTACC	422	22	62.17	50	
Reverse Primer	AGTGAGCATCCCTCTTTGAAC	532	21	62.16	47.62	
Product						111

Appendix Table 11: Transcript variants of *PGR*

Transcript Variant	**Similarity (%)**	**Number of base pairs**	**Query cover of alignment (%)**	**Base pair alignment range**
1	100	12 287	94	751 – 13 037
2	100	13 037	100	1 – 13 037
3	100	11 981	91	751 - 2651 2 954 – 13 037
7	100	10 957	84	87 - 387 2 381 – 13 037

All three transcript variants 1, 3 and 7 were 100% similar to transcript variant 2. Transcript variant 1 had the highest query cover (94%) when compared to transcript variant 2 which occurred between the region 751 – 13 037. Transcript variant 3 had a 91% alignment when compared to transcript variant 2. This alignment occurred over two regions; region 1 between 751 – 2 651 and region 2 between 2 954 – 13 037. Transcript variant 7 had the weakest alignment coverage (84%) when compared to transcript variant 2. The alignment and transcript variant 7 to transcript variant 7 was split over two regions; region 1 between 87 – 387 and region 2 between 2 381 and 13 037. The nucleotide sequence present in all four *PGR* transcript variants was 10 083 base pairs in length and found in the region of 2 954 – 13 037 on transcript variant 2. A BLAST search established that similarities of this sequence were limited to *PGR* and related sequences (Table 12).

Once it was established that the sequence was only similar to *PGR* transcript variants, the nucleotide sequence was analysed by PrimerQuest© (Integrated DNA Technologies). Subsequently, a BLAST search confirmed that the designed primers, when analysed as separate entities, were unique only to *PGR* transcript variants (Table 13).

Appendix Table 12: Designed forward and reverse primers for *PGR*

Type	Sequence	Start	Length (bp)	Tm (ºC)	GC (%)	Amplicon (bp)
Forward Primer	ATTACCAGTGTTCCCGTCTTC	7 436	21	61.85	47.62	
Reverse Primer	CCTGTACTTCCTCCAGCATAAG	7 546	22	61.80	50	
Product						111

References

Aghajanova, L., Horcajadas, J. A., Esteban, F. J. and Giudice, L. C. (2010) 'The Bone Marrow-Derived Human Mesenchymal Stem Cell: Potential Progenitor of the Endometrial Stromal Fibroblast1', *Biology of Reproduction*, 82(6), pp. 1076–1087. doi: 10.1095/biolreprod.109.082867.

Al-Asmakh, M. (2007) 'Reproductive functions of progesterone receptors.', *Recent Progress in Hormone Research*, 12(3), pp. 147–152. doi: 10.1210/rp.57.1.339.

Arends, M. J. (1999) 'Apoptosis in the endometrium', *Histopathology*, 35(2), pp. 174–178. doi: 10.1046/j.1365-2559.1999.00756.x.

Arnold, J. T., Kaufman, D. G., Seppälä, M. and Lessey, B. A. (2001) 'Endometrial stromal cells regulate epithelial cell growth in vitro: a new co-culture model.', *Human Reproduction (Oxford, England)*, 16(5), pp. 836–845.

Balasch, J. (2003) 'Sex steroids and bone: Current perspectives', *Human Reproduction Update*, 9(3), pp. 207–222. doi: 10.1093/humupd/dmg017.

Baulieu, É.-É. (1991) 'Neurosteroids: a new function in the brain', *Biology of the Cell*, 71(1), pp. 3–10.

Bazan, J. F. (1990) 'Haemopoietic receptors and helical cytokines', *Immunology Today*, 11(C), pp. 350–354. doi: 10.1016/0167-5699(90)90139-Z.

Bikfalvi, A. (2004) 'Platelet factor 4: an inhibitor of angiogenesis', *Seminars in Thrombosis and Hemostasis*, 30(3), pp. 379–385. doi: 10.1055/s-2004-831051.

Bochev, I., Belemezova, K., Shterev, A. and Kyurkchiev, S. (2016) 'Effect of cryopreservation on the properties of human endometrial stromal cells used in embryo co-culture systems', *Journal of Assisted Reproduction and Genetics*, 33(4), pp. 473–480. doi: 10.1007/s10815-016-0651-2.

Brar, A. K., Handwerger, S., Kessler, C. A. and Aronow, B. J. (2001) 'Gene induction and categorical reprogramming during in vitro human endometrial fibroblast decidualization.', *Physiological Genomics*, 7(2), pp. 135–48. doi: 10.1152/physiolgenomics.00061.2001.

Brosens, J. J., Pijnenborg, R. and Brosens, I. A. (2002) 'The myometrial junctional zone spiral arteries in normal and abnormal pregnancies', *American Journal of Obstetrics and Gynecology*,

187(5), pp. 1416–1423. doi: 10.1067/mob.2002.127305.

Bustin, S., Benes, V., Garson, J., Hellemans, J., Huggett, J., Kubista, M., Meuller, R., Nolan, T., Pfaffl, M., Shipley, G., Vandesompele, J. and Wittwer, C. (2009) 'The MIQE Guidelines: Minimum Information for Publication of Quantitative Real-Time PCR Experiments', *Clinical Chemistry*, 55(4), pp. 1–12. doi: 10.1373/clinchem.2008.112797.

Bustin, S. and Huggett, J. (2017) 'qPCR primer design revisited.', *Biomolecular Detection and Quantification*. Elsevier, 14(November), pp. 19–28. doi: 10.1016/j.bdq.2017.11.001.

Cai, G., Lai, B., Hong, H., Lin, P., Chen, W., Zhu, Z. and Chen, H. (2017) 'Effects of cryopreservation on excretory function, cellular adhesion molecules and vessel lumen formation in human umbilical vein endothelial cells', *Molecular Medicine Reports*, 16(1), pp. 547–552. doi: 10.3892/mmr.2017.6664.

Chatzaki, E., Kouimtzoglou, E., Margioris, A. N. and Gravanis, A. (2003) 'Transforming growth factor beta1 exerts an autocrine regulatory effect on human endometrial stromal cell apoptosis, involving the FasL and Bcl-2 apoptotic pathways.', *Molecular Human Reproduction*, 9(2), pp. 91–95. doi: 10.1093/molehr/gag011.

Chen, J. C., Hoffman, J. R., Arora, R., Perrone, L. A., Gonzalez-Gomez, C. J., Vo, K. C., Laird, D. J., Irwin, J. C. and Giudice, L. C. (2016) 'Cryopreservation and recovery of human endometrial epithelial cells with high viability, purity, and functional fidelity', *Fertility and Sterility*, 105(2), p. 501–510.e1. doi: 10.1016/j.fertnstert.2015.10.011.

Clarke, C. L. and Sutherland, R. L. (1990) 'Progestin Regulation of Cellular Proliferation', *Endocrine Reviews*, 11(2), pp. 266–301. doi: 10.1210/edrv-11-2-266.

Classen-Linke, I., Alfer, J., Hey, S., Krusche, C. A., Kusche, M. and Beier, H. M. (1998) 'Marker molecules of human endometrial differentiation can be hormonally regulated under in-vitro conditions as in-vivo', *Human Reproduction Update*, 4(5), pp. 539–549. doi: 10.1093/humupd/4.5.539.

Classen-Linke, I., Alfer, J., Krusche, C. A., Chwalisz, K., Rath, W. and Beier, H. M. (2000) 'Progestins, progesterone receptor modulators, and progesterone antagonists change VEGF release of endometrial cells in culture', *Steroids*, 65(10–11), pp. 763–771. doi: 10.1016/S0039-128X(00)00180-X.

Couse, J. F., Lindzey, J., Grandien, K., Gustafsson, J. A. and Korach, K. S. (1997) 'Tissue

distribution and quantitative analysis of estrogen receptor-alpha (ERalpha) and estrogen receptor-beta (ERbeta) messenger ribonucleic acid in the wild-type and ERalpha-knockout mouse.', *Endocrinology*, 138(11), pp. 4613–21. doi: 10.1210/endo.138.11.5496.

Dahlman-Wright, K., Cavailles, V., Fuqua, S. a, Jordan, V. C., Katzenellenbogen, J. a, Korach, K. S., Maggi, A., Muramatsu, M., Parker, M. G. and Gustafsson, J.-A. (2006) 'International Union of Pharmacology. LXIV. Estrogen receptors.', *Pharmacological Reviews*, 58(4), pp. 773–781. doi: 10.1124/pr.58.4.8.773.

Davar, R., Dehghani Firouzabadi, R. and Chaman Ara, K. (2013) 'Dilatation and curettage effect on the endometrial thickness', *Iranian Red Crescent Medical Journal*, 15(4), pp. 350–355. doi: 10.5812/ircmj.9863.

Deepak, S., Kottapalli, K., Rakwal, R., Oros, G., Rangappa, K., Iwahashi, H., Masuo, Y. and Agrawal, G. (2007) 'Real-Time PCR: Revolutionizing Detection and Expression Analysis of Genes.', *Current Genomics*, 8(4), pp. 234–51. doi: 10.2174/138920207781386960.

Deligdisch, L. (2000) 'Hormonal pathology of the endometrium.', *Modern pathology : an official journal of the United States and Canadian Academy of Pathology, Inc*, 13(3), pp. 285–294. doi: 10.1038/modpathol.3880050.

Deller, R. C., Vatish, M., Mitchell, D. A. and Gibson, M. I. (2014) 'Synthetic polymers enable non-vitreous cellular cryopreservation by reducing ice crystal growth during thawing.', *Nature Communications*. Nature Publishing Group, 5, p. 3244. doi: 10.1038/ncomms4244.

Dorman, B. H., Varma, V. A., Siegfried, J. M., Melin, S. A., Thomas, A., Norton, C. R., Kaufman, D. G., N, B. H. D., Varma, V. A., Siegfried, J. M., Melin, S. A., Adamec, T. A., Norton, C. R., Kaufman, D. G. and Hill, C. (1982) 'Morphology and Growth Potential of Stromal Cell Cultures Derived from Human Endometrium', *In Vitro*, 18(11), pp. 919–928.

Dunn, C. L., Kelly, R. W. and Critchley, H. O. D. (2003) 'Decidualization of the human endometrial stromal cell: an enigmatic transformation.', *Reproductive Biomedicine Online*. Reproductive Healthcare Ltd, Duck End Farm, Dry Drayton, Cambridge CB23 8DB, UK, 7(2), pp. 151–161. doi: 10.1016/S1472-6483(10)61745-2.

El-Khoury, V., Pierson, S., Kaoma, T., Bernardin, F. and Berchem, G. (2016) 'Assessing cellular and circulating miRNA recovery: The impact of the RNA isolation method and the quantity of input material', *Scientific Reports*. Nature Publishing Group, 6(January), pp. 1–14. doi: 10.1038/srep19529.

Fernández-Shaw, S., Shorter, S. C., Naish, C. E., Barlow, D. H. and Starkey, P. M. (1992) 'Isolation and purification of human endometrial stromal and glandular cells using immunomagnetic microspheres.', *Human Reproduction (Oxford, England)*, 7(2), pp. 156–161.

Fraser, H. M., Wilson, H., Silvestri, A., Morris, K. D. and Wiegand, S. J. (2008) 'The role of vascular endothelial growth factor and estradiol in the regulation of endometrial angiogenesis and cell proliferation in the marmoset', *Endocrinology*, 149(9), pp. 4413–4420. doi: 10.1210/en.2008-0325.

Freshney, R. I. (2005) 'Culture of Specific Cell Types', in *Culture of Animal Cells*, pp. 375–420. doi: 10.1002/0471747599.cac023.

Gao, J. (2000) 'Ligand-Activated Progesterone Receptor Isoform hPR-A Is a Stronger Transactivator Than hPR-B for the Expression of IGFBP-1 (Insulin-Like Growth Factor Binding Protein-1) in Human Endometrial Stromal Cells', *Molecular Endocrinology*, 14(12), pp. 1954–1961. doi: 10.1210/me.14.12.1954.

Gellersen, B. and Brosens, J. (2003) 'Cyclic AMP and progesterone receptor cross-talk in human endometrium: A decidualizing affair', *Journal of Endocrinology*, 178, pp. 357–372. doi: 10.1677/joe.0.1780357.

Genazzani, A. R., Stomati, M., Morittu, A., Bernardi, F., Monteleone, P., Casarosa, E., Gallo, R., Salvestroni, C. and Luisi, M. (2000) 'Progesterone, progestagens and the central nervous system.', *Human Reproduction (Oxford, England)*, 15 Suppl 1(April), pp. 14–27.

Ghatge, R. P., Jacobsen, B. M., Schittone, S. A. and Horwitz, K. B. (2005) 'The progestational and androgenic properties of medroxyprogesterone acetate: gene regulatory overlap with dihydrotestosterone in breast cancer cells', *Breast Cancer Research*, 7(6), p. R1036. doi: 10.1186/bcr1340.

Gibson, M. and Hammoud, A. O. (2013) *Clinical Reproductive Medicine and Surgery*. Edited by T. Falcone and W. W. Hurd. New York, NY: Springer New York. doi: https://doi.org/10.1007/978-3-319-52210-4_1.

Girling, J. E. and Rogers, P. A. W. (2005) 'Recent advances in endometrial angiogenesis research', *Angiogenesis*, 8(2), pp. 89–99. doi: 10.1007/s10456-005-9006-9.

Girling, J. E., Lederman, F. L., Walter, L. M. and Rogers, P. A. (2007) 'Progesterone, but not estrogen, stimulates vessel maturation in the mouse endometrium.', *Endocrinology* 148, pp.

5433-5441.

Girling, J. E. and Rogers, P. A. W. (2009) 'Regulation of endometrial vascular remodelling: Role of the vascular endothelial growth factor family and the angiopoietin-TIE signalling system', *Reproduction*, 138(6), pp. 883–893. doi: 10.1530/REP-09-0147.

Giulianelli, S., Vaqué, J. P., Soldati, R., Wargon, V., Vanzulli, S. I., Martins, R., Zeitlin, E., Molinolo, A. A., Helguero, L. A., Lamb, C. A., Gutkind, J. S. and Lanari, C. (2012) 'Estrogen receptor alpha mediates progestin-induced mammary tumor growth by interacting with progesterone receptors at the cyclin D1/MYC promoters', *Cancer Research*, 72(9), pp. 2416–2427. doi: 10.1158/0008-5472.CAN-11-3290.

Gold, L. I., Saxena, B., Mittal, K. R., Marmor, M., Goswami, S., Nactigal, L., Korc, M. and Demopoulos, R. I. (1994) 'Increased expression of transforming growth factor beta isoforms and basic fibroblast growth factor in complex hyperplasia and adenocarcinoma of the endometrium: evidence for paracrine and autocrine action.', *Cancer Research*, 54(9), pp. 2347–2358.

Gruber, C. J., Tschugguel, W., Schneeberger, C. and Huber, J. C. (2002) 'Production and actions of estrogens.', *The New England Journal of Medicine*, 346(5), pp. 340–52. doi: 10.1056/NEJMra000471.

Gruber, D. and Jayme, D. (1994) 'Cell and Tissue Culture Media: History and Terminology', in *Cell Biology: A Laboratory Handbook*, pp. 451–458. doi: doi.org/10.1016/B978-0-12-164717-9.50059-3.

Gupta, M. K. and Chia, S.-Y. (2013) 'Ovarian Hormones: Structure, Biosynthesis, Function, Mechanism of Action, and Laboratory Diagnosis', in Falcone, T. and Hurd, W. W. (eds) *Clinical Reproductive Medicine and Surgery: A Practical Guide*. New York, NY: Springer New York, pp. 1–30. doi: 10.1007/978-1-4614-6837-0_1.

Harrison, R. G., Greenman, M. J., Mall, F. P. and Jackson, C. M. (1907) 'Observations of the living developing nerve fiber', *The Anatomical Record*, 1(5), pp. 116–128. doi: 10.1002/ar.1090010503.

Huang, J., Liu, D. and Dawood, M. Y. (1998) 'The expression of vascular endothelial growth factor isoforms in cultured human endometrial stromal cells and its regulation by 17 β -oestradiol', *Molecular Human Reproduction*, 4(6), pp. 603–607.

Hunt, J. (2006) ‘A Stranger in a Strange Land’, *Immunological Reviews*, 213, pp. 36–47.

Isachenko, V., Isachenko, E., Mallmann, P. and Rahimi, G. (2013) ‘Increasing follicular and stromal cell proliferation in cryopreserved human ovarian tissue after long-term precooling prior to freezing: In vitro versus chorioallantoic membrane (CAM) xenotransplantation’, *Cell Transplantation*, 22(11), pp. 2053–2061. doi: 10.3727/096368912X658827.

Jabbour, H. N. and Critchley, H. O. D. (2001) ‘Potential roles of decidual prolactin in early pregnancy’, *Reproduction*, 121(2), pp. 197–205. doi: 10.1530/rep.0.1210197.

Jensen, F., Woudwyk, M., Teles, A., Woidacki, K., Taran, F., Costa, S., Malfertheiner, S. F. and Zenclussen, A. C. (2010) ‘Estradiol and progesterone regulate the migration of mast cells from the periphery to the uterus and induce their maturation and degranulation’, *PLoS ONE*, 5(12), pp. 1–12. doi: 10.1371/journal.pone.0014409.

Jones, R. L., Stoikos, C., Findlay, J. K. and Salamonsen, L. a. (2006) ‘TGF-β superfamily expression and actions in the endometrium and placenta’, *Reproduction*, 132, pp. 217–232. doi: 10.1530/rep.1.01076.

Kajihara, T., Brosens, J. J. and Ishihara, O. (2013) ‘The role of FOXO1 in the decidual transformation of the endometrium and early pregnancy’, *Medical Molecular Morphology*, 46, pp. 61–68. doi: 10.1007/s00795-013-0018-z.

Kamada, M., Yamano, S. and Irahara, M. (1997) ‘Estrogen, progesterone: biosynthesis, receptor and action’, *Nihon Rinsho*, 55, pp. 2865–2870.

Kastner, P., Krust, A., Turcotte, B., Stropp, U., Tora, L., Gronemeyer, H. and Chambon, P. (1990) ‘transcripts encoding the two functionally different human progesterone receptor forms A and B’, *The EMBO Journal*, 9(5), pp. 1603–1614.

Kim, M. G., Shim, J. Y., Pak, J. H., Jung, B. K., Won, H. S., Lee, P. R. and Kim, A. (2012) ‘Progesterone Modulates the Expression of Interleukin-6 in Cultured Term Human Uterine Cervical Fibroblasts’, *American Journal of Reproductive Immunology*, 67(5), pp. 369–375. doi: 10.1111/j.1600-0897.2011.01094.x.

King, T. and Brucker, M. (2011) *Pharmacology for women’s health*. 1st ed. Massachusetts: Jones and Bartlett.

Kishimoto, T. (2010) ‘IL-6: From its discovery to clinical applications’, *International Immunology*, 22(5), pp. 347–352. doi: 10.1093/intimm/dxq030.

Koukourokis, M. I., Giatromanolaki, A., Sivridis, E., Simopoulos, C., Gatter, K. C., Harris, A. L. and Jackson, D. G. (2005) 'LYVE-1 immunohistochemical assessment of lymphagiogenesis in endometrial and lung cancer', *Journal of Clinical Pathology*, 58(2), pp. 202–206. doi: 10.1136/jcp.2004.019174.

Kralik, P. and Ricchi, M. (2017) 'A basic guide to real time PCR in microbial diagnostics: Definitions, parameters, and everything', *Frontiers in Microbiology*, 8(FEB), pp. 1–9. doi: 10.3389/fmicb.2017.00108.

Krikun, G., Mor, G., Alvero, A., Guller, S., Schatz, F., Sapi, E., Rahman, M., Caze, R., Qumsiyeh, M. and Lockwood, C. J. (2004) 'A novel immortalized human endometrial stromal cell line with normal progestational response', *Endocrinology*, 145(5), pp. 2291–2296. doi: 10.1210/en.2003-1606.

Kuiper, G. G., Carlsson, B., Grandien, K., Enmark, E., Häggblad, J., Nilsson, S. and Gustafsson, J. A. (1997) 'Comparison of the ligand binding specificity and transcript tissue distribution of estrogen receptors alpha and beta.', *Endocrinology*, 138(3), pp. 863–70. doi: 10.1210/endo.138.3.4979.

Larsen, B. and Monif, G. R. G. (2001) 'Understanding the Bacterial Flora of the Female Genital Tract', *Clinical Infectious Diseases*, 32(4), pp. e69–e77. doi: 10.1086/318710.

Logan, P. C., Ponnampalam, A. P., Steiner, M. and Mitchell, M. D. (2013) 'Effect of cyclic amp and estrogen/progesterone on the transcription of dna methyltransferases during the decidualization of human endometrial stromal cells', *Molecular Human Reproduction*, 19(5), pp. 302–312. doi: 10.1093/molehr/gas062.

Luginbuhl, W. H. (1968) 'Electron microscopic study of the effects of tissue culture on human endometrium', *American Journal of Obstetrics and Gynecology*, 102(2), pp. 192–201. doi: 10.1016/0002-9378(68)90318-9.

Massagué, J., Andres, J., Attisano, L., Cheifetz, S., López-Casillas, F., Ohtsuki, M. and Wrana, J. L. (1992) 'TGF-β receptors', *Molecular Reproduction and Development*, 32(2), pp. 99–104. doi: 10.1002/mrd.1080320204.

Mattei, M. G., Borg, J. P., Rosnet, O., Marmé, D., Birnbaum, D., Chromosome, H. and Marme, D. (1996) 'Assignment of vascular endothelial growth factor (VEGF) and placenta growth factor (PLGF) genes to human chromosome 6p12-p21 and 14q24-q31 regions, respectively.', *Genomics*, 32(1), pp. 168–9. doi: 10.1006/geno.1996.0098.

Matthews, C. J., Redfern, C. P., Hirst, B. H. and Thomas, E. J. (1992) 'Characterization of human purified epithelial and stromal cells from endometrium and endometriosis in tissue culture.', *Fertility and Sterility*. Elsevier Masson SAS, 57(5), pp. 990–997. doi: S0015-0282(16)55014-6 [pii].

McDonnell, D. P. and Goldman, M. E. (1994) 'RU486 exerts antiestrogenic activities through a novel progesterone receptor A form-mediated mechanism', *Journal of Biological Chemistry*, 269(16), pp. 11945–11949. doi: 8163495.

Mote, P. A., Balleine, R. L., McGowan, E. M. and Clarke, C. L. (1999) 'Colocalization of progesterone receptors a and b by dual immunofluorescent histochemistry in human endometrium during the menstrual cycle', *Journal of Clinical Endocrinology and Metabolism*, 84(8), pp. 2963–2971. doi: 10.1210/jc.84.8.2963.

Mulac-Jericevic, B. and Conneely, O. M. (2004) 'Reproductive tissue selective actions of progesterone receptos', *Reproduction*, 128(2), pp. 139–146. doi: 10.1530/rep.1.00189.

Nilsson, S., Mäkelä, S., Treuter, E., Tujague, M., Thomsen, J., Andersson, G., Enmark, E., Pettersson, K., Warner, M. and Gustafsson, J. A. (2001) 'Mechanisms of estrogen action.', *Physiological Reviews*, 81(4), pp. 1535–65. Available at: http://www.ncbi.nlm.nih.gov /pubmed/11581496.

Nishida, M. (2002) 'The Ishikawa cells from birth to the present.', *Human cell : Official Journal of Human Cell Research Society*, 15(3), pp. 104–117. doi: 10.1111/j.1749-0774.2002.tb00105.x.

Nishida, M., Kasahara, K., Kaneko, M. and Al., E. (1985) 'Establishment of a new human endometrial adenocarcinoma cell line, Ishikawa cells, containing estrogen and progesterone receptors', *Nihon Sanka Fujinka Gakkai Zasshi*, 37, pp. 1103–1111.

Ohno, Y. and Fujimoto, Y. (1998) 'Endometrial oestrogen and progesterone receptors and their relationship to sonographic appearance of the endometrium', *Human Reproduction Update*, 4(5), pp. 560–564.

Osteen, K. G., Hill, G. A., Hargrove, J. T. and Gorstein, F. (1989) 'Development of a method to isolate and culture highly purified populations of stromal and epithelial cells from human endometrial biopsy specimens', *Fertility and Sterility*. Elsevier Masson SAS, 52(6), pp. 965–972. doi: 10.1016/S0015-0282(16)53160-4.

Qiagen (2010) *Critical Factors for Successful Real-Time PCR*. Available at: https://www.qiagen.com/br/resources/resourcedetail?id=f7efb4f4-fbcf-4b25-9315-c4702414e8d6&lang=en.

Ren, C.-E., Zhu, X., Li, J., Lyle, C., Dowdy, S., Podratz, K., Byck, D., Chen, H.-B. and Jiang, S.-W. (2015) 'Microarray Analysis on Gene Regulation by Estrogen, Progesterone and Tamoxifen in Human Endometrial Stromal Cells', *International Journal of Molecular Sciences*, 16(3), pp. 5864–5885. doi: 10.3390/ijms16035864.

Rizk, B., Aboulghar, M., Smitz, J. and Ron-El, R. (1997) 'The role of vascular endothelial growth factor and interleukins in the pathogenesis of severe ovarian hyperstimulation syndrome.', *Human Reproduction Update*, 3(3), pp. 255–66. doi: 10.1093/humupd/3.3.255.

Robertson, J. M. and Walsh-Weller, J. (1998) 'An introduction to PCR primer design and optimization of amplification reactions.', *Methods in Molecular Biology (Clifton, N.J.)*, 98(12), pp. 121–54. doi: 10.1385/0-89603-443-7:121.

Ross, M. and Pawlina, W. (2006) *Histology: A text and atlas*. 5th ed. Baltimore: Lippincott Williams & Wilkins.

Ryan, J. (2004) 'General guide for cryogenically storing animal cell cultures', *Technical Information/Cell Culture* pp. 1–10. Available at: http://catalog2.corning.com /Lifesciences/media/pdf/t_cryoanimalcc.pdf.

Ryan, K. J. (1982) 'Biochemistry of Aromatase : Significance to Female Reproductive Physiology Biochemistry of Aromatase : Significance to Female Reproductive', *Cancer Research*, 42(August), pp. 3342–3345.

Samalecos, A. and Gellersen, B. (2008) 'Systematic expression analysis and antibody screening do not support the existence of naturally occurring progesterone receptor (PR)-C, PR-M, or other truncated PR isoforms', *Endocrinology*, 149(11), pp. 5872–5887. doi: 10.1210/en.2008-0602.

Sander, C. and Schneider, R. (1991) 'Database of homology???derived protein structures and the structural meaning of sequence alignment', *Proteins: Structure, Function, and Bioinformatics*, 9(1), pp. 56–68. doi: 10.1002/prot.340090107.

Santoro, N., Worsley, R., Miller, K. K., Parish, S. J. and Davis, S. R. (2016) 'Role of Estrogens and Estrogen-Like Compounds in Female Sexual Function and Dysfunction', *Journal of Sexual*

Medicine. Elsevier Inc, 13(3), pp. 305–316. doi: 10.1016/j.jsxm.2015.11.015.

Satyaswaroop, P. G., Bressler, R. S., de la Pena, M. M. and Gurpide, E. (1979) 'Isolation and culture of human endometrial glands', *The Journal of Clinical Endocrinology and Metabolism*, 48(4), pp. 639–641. doi: 10.1210/jcem-48-4-639.

Senger, D. R., Galli, S. J., Dvorak, A. M., Perruzzi, C. A., Harvey, V. S. and Dvorak, H. F. (1983) 'Tumor cells secrete a vascular permeability factor that promotes accumulation of ascites fluid.', *Science (New York, N.Y.)*, 219(4587), pp. 983–5. doi: 6823562.

Sharkey, A. M., Day, K., Pherson, A. M. C., Malik, S., Licence, D. and Smith, S. K. (2000) 'Vascular Endothelial Growth Factor Expression in Human Endometrium Is Regulated by Hypoxia.', *The Journal of Clinical Endocrinology and Metabolism*, 85(1), pp. 402–409.

Sheridan, G. E. C., Masters, C. I., Shallcross, J. A. and Mackey, B. M. (1998) 'Detection of mRNA by Reverse Transcription-PCR as an Indicator of Viability in Escherichia coliCells Detection of mRNA by Reverse Transcription-PCR as an Indicator of Viability in Escherichia coli Cells', *Applied and Environmental Microbiology*, 64(4), pp. 1313–1318.

Sherman, D. (1999) 'Uterine flora at cesarean and its relationship to postpartum endometritis.', *Obstetrics & Gynecology*, 94(5), pp. 787–791. doi: 10.1016/S0029-7844(99)00421-4.

Simoncini, T., Scorticati, C., Mannella, P., Fadiel, A., Giretti, M. S., Fu, X. D., Baldacci, C., Garibaldi, S., Caruso, A., Fornari, L., Naftolin, F. and Genazzani, A. R. (2006) 'Estrogen receptor alpha interacts with Galpha13 to drive actin remodeling and endothelial cell migration via the RhoA/Rho kinase/moesin pathway.', *Molecular Endocrinology*, 20(8), pp. 1756-1771. doi: 10.1210/me.2005-0259

Spitzer, T. L. B., Rojas, a., Zelenko, Z., Aghajanova, L., Erikson, D. W., Barragan, F., Meyer, M., Tamaresis, J. S., Hamilton, a. E., Irwin, J. C. and Giudice, L. C. (2012) 'Perivascular Human Endometrial Mesenchymal Stem Cells Express Pathways Relevant to Self-Renewal, Lineage Specification, and Functional Phenotype', *Biology of Reproduction*, 86(November 2011), pp. 58–58. doi: 10.1095/biolreprod.111.095885.

Srivastava, A., Sengupta, J., Kriplani, A., Roy, K. K. and Ghosh, D. (2013) 'Profiles of cytokines secreted by isolated human endometrial cells under the influence of chorionic gonadotropin during the window of embryo implantation.', *Reproductive Biology and Endocrinology : RB&E*, 11, p. 116. doi: 10.1186/1477-7827-11-116.

Stevenson, S., Nelson, L. D., Sharpe, D. T. and Thornton, M. J. (2008) '17β-Estradiol regulates the secretion of TGF-β by cultured human dermal fibroblasts', *Journal of Biomaterials Science, Polymer Edition*, 19(8), pp. 1097–1109. doi: 10.1163/156856208784909354.

Stoikos, C. J., Harrison, C. A., Salamonsen, L. A. and Dimitriadis, E. (2008) 'A distinct cohort of the TGFβ superfamily members expressed in human endometrium regulate decidualization', *Human Reproduction*, 23(6), pp. 1447–1456. doi: 10.1093/humrep/den110.

Szóstek, A. Z., Siemieniuch, M. J., Galvão, A. M., Lukasik, K., Zieba, D., Ferreira-Dias, G. M. and Skarzynski, D. J. (2012) 'Effects of cell storage and passage on basal and oxytocin-regulated prostaglandin secretion by equine endometrial epithelial and stromal cells', *Theriogenology*. Elsevier Inc., 77(8), pp. 1698–1708. doi: 10.1016/j.theriogenology.2011.12.015.

Tabanelli, S., Tang, B. and Gurpldet, E. (1992) 'in Vitro Decidualization of Human Endometrial Stromal Cells', *Molecular Biology*, 424(3), pp. 337–344. doi: 10.1016/0960-0760(92)90137-8.

Tabibzadeh, S. (1998) 'Molecular control of the implantation window', *Human Reproduction Update*, 4(5), pp. 465–471. doi: 10.1093/humupd/4.5.465.

Tabibzadeh, S. S., Santhanam, U., Sehgal, P. B. and May, L. T. (1989) 'Cytokine-induced production of IFN-beta 2 / IL-6 by freshly explanted human endometrial stromal cells . Modulation by estradiol-17 beta', *The Journal of Immunology*, 142(9), pp. 3134–3139.

Takahashi, T., Eitzman, B., Bossert, N. L., Walmer, D., Sparrow, K., Flanders, K. C., McLachlan, J. and Nelson, K. G. (1994) 'Transforming growth factors beta 1, beta 2, and beta 3 messenger RNA and protein expression in mouse uterus and vagina during estrogen-induced growth: a comparison to other estrogen-regulated genes', *Cell Growth & Differentiation*, 5(9), pp. 919–935. Available at: http://cgd.aacrjournals.org/cgi/reprint/5/9/919.pdf.

Trenti, A., Tedesco, S., Boscaro, C., Trevisi, L., Bolega, C. and Cignarella, A. (2018) 'Estrogen, Angiogenesis, Immunity and Cell Metabolism: Solving the Puzzle.', *International Journal of Molecular Sciences*, 19(3), pp. 859. doi: 10.3390/ijms19030859.

Trundley, A., Gardner, L., Northfield, J., Chang, C. and Moffett, A. (2006) 'Methods for isolation of cells from the human fetal-maternal interface.', *Methods in Molecular Medicine*, 122, pp. 109–22. doi: 10.1385/1-59259-989-3.

Valasek, M. A. (2005) 'The power of real-time PCR', *AJP: Advances in Physiology Education*, 29(3), pp. 151–159. doi: 10.1152/advan.00019.2005.

Varma, V. A., Melin, S. A., Adamec, T. A., Dorman, B. H., Siegfried, J. M., Walton, L. A., Carney, C. N., Norton, C. R. and Kaufman, D. G. (1982) 'Monolayer culture of human endometrium: Methods of culture and identification of cell types', *In Vitro*, 18(11), pp. 911–918. doi: 10.1007/BF02796347.

Vegeto, E., Shahbaz, M. M., Wen, D. X., Goldman, M. E., O'Malley, B. W. and McDonnell, D. P. (1993) 'Human progesterone receptor A form is a cell- and promoter-specific repressor of human progesterone receptor B function.', *Molecular Endocrinology*, 7(10), pp. 1244–1255. doi: 10.1210/mend.7.10.8264658.

Vereide, A. B., Kaino, T., Sager, G., Arnes, M. and Ørbo, A. (2006) 'Effect of levonorgestrel IUD and oral medroxyprogesterone acetate on glandular and stromal progesterone receptors (PRA and PRB), and estrogen receptors (ER-α and ER-β) in human endometrial hyperplasia', *Gynecologic Oncology*, 101(2), pp. 214–223. doi: 10.1016/j.ygyno.2005.10.030.

Vierck, J. L., Byrne, K., Mir, P. S. and Dodson, M. V. (1999) 'Ten commandments for preventing contamination of primary cell cultures', *Methods in Cell Science*, 22(1), pp. 33–41. doi: 10.1023/A:1009826012986.

Vierck, J. L. and Dodson, M. V. (1999) 'Interpretation of cell culture phenomena', *Methods in Cell Science*, 22(1), pp. 79–81. doi: 10.1023/A:1009873912078.

Viet-Phuong Le, A., Huang, D., Blick, T., Thompson, E. W. and Dobrovic, A. (2015) 'An optimised direct lysis method for gene expression studies on low cell numbers', *Scientific Reports*. Nature Publishing Group, 5(1), p. 12859. doi: 10.1038/srep12859.

Weinstein, M. P. and Weinstein, M. P. (2003) 'Blood Culture Contamination : Persisting Problems and Partial Progress MINIREVIEW Blood Culture Contamination : Persisting Problems and Partial Progress', 41(6), pp. 2275–2278. doi: 10.1128/JCM.41.6.2275.

Von Wolff, M., Thaler, C. J., Zepf, C., Becker, V., Beier, H. M. and Strowitzki, T. (2002) 'Endometrial expression and secretion of interleukin-6 throughout the menstrual cycle', *Gynecological Endocrinology*, 16(2), pp. 121–129. doi: 10.1080/gye.16.2.121.129.

Zhang, L., Rees, M. C. and Bicknell, R. (1995) 'The isolation and long-term culture of normal human endometrial epithelium and stroma. Expression of mRNAs for angiogenic polypeptides

basally and on oestrogen and progesterone challenges.', *Journal of cell science*, 108 (Pt 1, pp. 323–31. Available at: http://www.ncbi.nlm.nih.gov/pubmed/7537745.

Zumbo, P. (no date) *Ethanol Precipitation*. Available at: http://physiology.med.cornell.edu/faculty/mason/lab/zumbo/files/ETHANOL_PRECIPITATION.pdf.

540501:Dissertation_4pm_1_April.docx

ORIGINALITY REPORT

9%	7%	6%	4%
SIMILARITY INDEX	INTERNET SOURCES	PUBLICATIONS	STUDENT PAPERS

PRIMARY SOURCES

1	orca.cf.ac.uk Internet Source	1%
2	diabetes.diabetesjournals.org Internet Source	<1%
3	Submitted to University of Huddersfield Student Paper	<1%
4	Submitted to University of Aberdeen Student Paper	<1%
5	Submitted to Texas Christian University Student Paper	<1%
6	Gary S. Lazar, Laima Gaidulis, Michael Henke, Karl G. Blume. "A sensitive screening method of detecting anti-granulocyte antibodies employing radiolabeled staphylococcal protein A", Journal of Immunological Methods, 1984 Publication	<1%
7	Submitted to University of Leicester Student Paper	<1%
	"Scientific Abstracts", Journal of the Society for	